



UNIVERSITAT
POLITÈCNICA
DE VALÈNCIA



UNIVERSITAT POLITÈCNICA DE VALÈNCIA

School of Industrial Engineering

Study of the applications of fused filament fabrication with
conductive materials. Analysis of operational problems.

End of Degree Project

Bachelor's Degree in Industrial Engineering

AUTHOR: Rondou, Thomas

Tutor: Gutiérrez Rubert, Santiago Carlos

Cotutor: Lluch Cerezo, Joaquín

ACADEMIC YEAR: 2023/2024



UNIVERSITAT
POLITÈCNICA
DE VALÈNCIA



ESCUELA TÉCNICA
SUPERIOR INGENIERÍA
INDUSTRIAL VALENCIA

Bachelor's degree in industrial engineering

STUDY OF APPLICATIONS OF FUSED FILAMENT FABRICATION WITH CONDUCTIVE MATERIALS. ANALYSIS OF OPERATIONAL PROBLEMS.

AUTHOR: THOMAS RONDOU

TUTORS: SANTIAGO C. GUTIÉRREZ RUBERT

JOAQUIN LLUCH CEREZO

Academic year: 2023-2024

Abstract

Study of applications of fused filament fabrication with conductive materials. Analysis of operational problems.

T. Rondou

Additive manufacturing, better known as 3d-printing, offers a unique and affordable solution for the production of complex geometries with high tolerances. The combination of this manufacturing method with conductive polymers can enable low-cost prototyping for a myriad of applications.

In this study, the potential application domains where Fused Filament Fabrication parts, fabricated using flexible conductive materials such as thermoplastic polyurethane, can play a pivotal role are examined. The focus will be on practical scenarios where additive manufacturing and conductive polymers intersect.

Keywords: Additive manufacturing, Fused Filament Fabrication, Conductive polymers, Printed conductive applications

Table of contents

List of figures.....	7
List of tables.....	8
Introduction	9
1 Literature study.....	11
1.1 Behavior of conductive polymers.....	11
1.2 3D printing method	12
1.3 FDM applications of conductive polymers	14
1.3.1 Loadcells	14
1.3.2 Safety applications.....	15
1.3.3 Flexible and stretchable electronics.....	15
1.3.4 Antennas.....	15
1.3.5 Universal conducting module	17
1.4 Sustainable development goals.....	17
1.4.1 SDG 8: Decent work and economic growth	17
1.4.2 SDG 9: Industry, innovation and infrastructure.....	17
1.4.3 SDG 12: Responsible consumption and production	17
2 Preliminary study.....	18
2.1 Clarification test sample	18
2.2 Encountered problems	19
2.2.1 Origin orientation.....	19
2.2.2 “Blobby” zones	19
2.2.3 Mixing problem	19
2.2.4 Design issue.....	19
2.3 Print parameters.....	20
2.3.1 Non-conductive TPU	20
2.3.2 Conductive TPU.....	21
2.3.3 Combination of conductive TPU with non-conductive TPU.....	23
2.3.4 Combination of conductive TPU with PLA.....	23
3 Chosen applications.....	25
3.1 Circuit board	25
3.1.1 Design and methodology	25
3.1.2 Problems and results	25
3.2 Strain Gauge.....	27
3.2.1 Methodology.....	27
3.2.2 Arduino setup test.....	27
3.2.3 Design of sample	28

3.2.4	Pretesting the samples.....	29
3.2.5	Results.....	30
3.3	Antenna.....	32
3.3.1	Design	32
3.3.2	Printing of the antenna.....	32
3.3.3	Methodology.....	35
3.3.4	Results.....	36
4	Material behavior.....	38
4.1	Methodology.....	38
4.2	Results.....	38
4.2.1	Decreasing resistance.....	38
4.2.2	Consistency	39
4.2.3	Extra investigation on retraction	39
4.2.4	Extra investigation on printing temperature.....	40
5	Design of Experiments.....	41
5.1	Testing parameters	41
5.2	Sample design	42
5.3	ANOVA study	43
5.3.1	Measurement	43
5.3.2	Statistic problems	43
5.3.3	Results.....	44
6	Economic study and budget	46
6.1	Cost of used material.....	46
6.2	Cost of machines	46
6.2.1	Ultimaker 3 Extended	46
6.2.2	Instron 5967.....	46
6.2.3	NanoVNA h4	46
6.3	Cost of licenses	47
6.4	Labor cost.....	47
6.5	Total cost.....	47
	Conclusion.....	49
	Bibliography.....	51
	List of appendices	53

List of figures

Figure 1: Schematic arrangement of the FFF process	13
Figure 2: Extrusion systems: Bowden tubes vs direct drive	13
Figure 3: Universal conducting modules	17
Figure 4: Example of parameters that can be modified in Cura.....	18
Figure 5: Test sample for test of change in conductivity.....	19
Figure 6: Test prints of not conductive material: (a) 45 mm/s (b) 35 mm/s (c) 25 mm/s and (d) 25 mm/s + 120%/130% flowrate	21
Figure 7: Obstruction in extruder	21
Figure 8: Test prints conductive TPU: (a) extruder pressure problems, (b) best parameters and (c) new print core	22
Figure 9: Print core issue, darker communication wires.....	22
Figure 10: Experiments combining materials: (a) previously determined settings, (b) reduced speed, increased heat and flow, (c) further increased flow and decreased speed.....	23
Figure 11: Combination conductive TPU with PLA: (a) parameters and (b) with "Nozzle Switch Extra Prime Amount" setting on.....	24
Figure 12: (a) line distance 0,6 mm and (b) line distance 0,5 mm	24
Figure 13: (a) Electrical diagram and (b) Experimental setup on breadboard	25
Figure 14: (a) Top view, (b) Non-conductive bottom layer and (c) bottom layer with conductive connections.....	26
Figure 15: (a) with adapter piece and (b) without adapter piece, final result	26
Figure 16: Voltage divider Arduino setup.....	27
Figure 17: Resistance in function of time using a variable resistor.....	28
Figure 18: Model of a standard linear strain gauge	28
Figure 19: Design of strain gauge	29
Figure 20: Connections between conductive lines	29
Figure 21: Sample 1 (a) and sample 2 (b) in Instron machine.....	30
Figure 22: Resistance in function of time sample 1	30
Figure 23: Graph of resistance in function of extension sample 2.....	31
Figure 24: Patch antenna design and dimensions in millimeters (Striker et al., 2020)	32
Figure 25: Test one (a) and two (b) of printing the antenna	33
Figure 26: Result after iteration of parameters	33
Figure 27: (a) Result after ironing (b) Results after manual manipulation.....	34
Figure 28: SMA-RP connector on antenna.....	34
Figure 29: Antenna connected to VNA	36
Figure 30: Measured return loss.....	36
Figure 31: Comparison internal receiver vs printed antenna	37
Figure 32: Decreasing resistance in function of time.....	39
Figure 33: DoE sample design (dimensions in millimeters).....	42
Figure 34: Visualization of "per model setting"	43
Figure 35: Result of collinearity test.....	44
Figure 36: Results of one-way ANOVA studies	44
Figure 37: Visualization variables	45

List of tables

- Table 1: Relation Between Return Loss, Power % Reflected Back and VSWR 35
- Table 2: Print parameters samples 38
- Table 3: Results of consistency test 39
- Table 4: Results of different retraction distances..... 40
- Table 5: Results of different printing temperatures 40
- Table 6: Values of fixed parameter 41
- Table 7: Amount and dispersion of experiments 42
- Table 8: Resistance of the samples 43
- Table 9: Cost of the used material 46
- Table 10: Breakdown of project cost and total..... 47

Introduction

The motivation for this paper arises from the rapid advancement of 3D printing technology, particularly Fused Filament Fabrication (FFF), which has opened new possibilities for the fabrication of functional devices. The use of conductive materials in FFF has gained significant interest, especially in the fields of electronics and sensor technology. However, there are still many challenges and operating problems associated with the use of conductive materials in FFF printing. This final degree project aims to address these issues, focusing on a few selected typical examples, like WIFI antennas and strain gauges.

The primary objective of this project is to study the operating problems associated with FFF printed applications using conductive materials in a commercial 3D printer. This includes investigating the current state of FFF printing with conductive materials, analyzing the operating problems associated with it and proposing solutions or improvements to mitigate these operating problems. This while evaluating the performance of the improved FFF printed applications in terms of functionality, reliability, and durability.

The research method for the project is a literature study of various applications and materials. The primary sources are scientific papers from related studies. Subsequently, a preliminary study is conducted to identify the properties and potential printing issues of the selected material. This allows for the optimization of print parameters to achieve the best print quality. In the third chapter, various applications are examined to determine their suitability for this type of material. The fourth and fifth chapters focus on further investigation into the behavior of two types of conductive polymers. Finally, an economic analysis related to this project is performed, and the findings are summarized in the conclusion.

By achieving these objectives, this thesis aims to contribute to the advancement of FFF printing technology and its applications in the field of electronics and sensor technology. The findings of this study are expected to provide valuable insights for researchers, engineers, and manufacturers working in this field.

1 Literature study

1.1 Behavior of conductive polymers

Ryan et al. (2022) provides an overview of significant advancements in additively manufactured conductive polymers and nanocomposites, highlighting their potential applications in various fields such as bioelectronics, flexible electronics, sensors, and electrochemical devices. The ability to additively manufacture these materials enables the creation of lightweight, conductive, and intricate designs, expanding the possibilities within the additive manufacturing industry beyond traditional prototyping. Key areas of discussion include enhancing nanoparticle dispersion for uniform printing and improving the balance between electrical conductivity and mechanical properties. Incorporating a secondary polymer shows promise for achieving desired mechanical strength alongside conductivity. While the literature demonstrates promising electrical conductivities, the ability of additively manufactured conductive polymers and nanocomposites to compete with metal components remains uncertain. However, with the progress in additive manufacturing technologies, significant improvements in both electrical and mechanical properties are promising for the future.

Beniak et al. (2020) tested conductive PLA (Polylactic acid) material using FDM (Fused Deposition Modeling) Additive Manufacturing technology. The primary objectives of these experiments are to determine the strength of the produced samples and to assess their essential electrical properties which will affect the preliminary study of this project.

The most significant factor affecting tensile strength testing is the infill volume. This observation aligns with findings from various scientific papers. Beniak et al. (2015) claims that the layer direction has a huge impact on the strength of the sample. Additionally, the type of infill has a crucial role. Specifically, the rectilinear infill exhibits greater strength in this experiment compared to the honeycomb infill. While honeycomb structures are generally better suited for compression loads, the specimens in this study are subjected to tensile loads.

The third factor, layer height, has less impact than the previous two. It's essential to understand the tensile strength, which was measured during testing. The highest value achieved in the experiments was 32 MPa with 90% infill. However, they anticipate that the tensile strength of a 100% infill specimen would be even higher, possibly reaching 42 MPa.

Regarding resistivity, they explored the relation between the length of produced specimens and their resistivity. This factor is important related to the study done in this paper. Based on Ohm's law and the experiments, there is found that this relation is linear due to more conductive material in longer specimens.

Interestingly, the nozzle temperature during 3D printing significantly effects resistivity. At a higher temperature of 220°C, the measured resistivity values are considerably lower. This discrepancy, approximately 30%, is attributed to structural changes within the material.

Developing 3D printed objects incorporating embedded 3D printed electronic circuits using electrically conductive filament is an achievable objective for FFF 3D printers. Jaksic & Desai (2018) focused on the creation of the simplest electrical passive element, the resistor. The resistors produced using graphene-based filament exhibit non-homogeneous characteristics due to the FFF process, resulting in varying resistivity based on build orientation and process parameters. Employing an FFF printer equipped with two extruders and specialized software, a series of resistors were fabricated for characterization. Expansion along the x-axis led to increased resistivity, albeit nonlinearly. Conversely, resistivity increased linearly with z-axis expansions. This

study offers guidelines and recommendations for designing 3D printed resistors as integral components of 3D printed objects containing electrical circuits.

This final degree project involves several key aims. Foremost among these is the goal to merge conductive components within intricate geometric structures at a cost-effective rate. This involves utilizing TPU (thermoplastic polyurethane) as a conductive material, presenting a versatile approach with potential applications across various domains. Additionally, there is a concerted effort to examine how different 3D printing parameters influence the final conductivity of the printed parts, offering valuable insights into optimization strategies. Another aspect involves confirming the practicality of joining TPU with traditional low temperature welding alloys, thereby enhancing the technology's versatility and applicability in real-world scenarios. Each of these aims highlights the project's dedication to innovation, efficiency, and practicality within the fields of additive manufacturing and material science.

Aloqalaa (2022) investigated several conductive filaments and their applications. Due to its good flexibility and relative low resistance, the conductive TPU used in this study is Filaflex Conductive, manufactured by Recreus (Appendix 1). The TPU becomes conductive due to the addition of fillers or nanofillers. A common strategy involves blending pure polymers with electrically conductive fillers, such as metals and carbon-based nanofillers making the filament conductive. Metallic options encompass copper, nickel, gold, and silver, available in powder, flake, coated fiber, and nanowire formats. Carbon-based alternatives range from carbon nanotubes and fibers to graphene and carbon black. This amalgamation yields conductive polymer composites, often featured in literature, boasting resistivities bridging the gap between metallic conductors ($10^{-7} \Omega\text{m}$) and insulating materials ($10^{25} \Omega\text{m}$). The type of filler for the Conductive Filaflex is not specified by the manufacturer (Maldonado et al., 2022; Misiak et al., 2024).

1.2 3D printing method

Fused Filament Fabrication (FFF), also known as Fused Deposition Modeling (FDM), is a popular additive manufacturing (AM) process used to create three-dimensional objects. In FFF printing, a plastic filament is fed through a heated extruder nozzle, where it is melted and deposited layer by layer onto a build platform as shown in Figure 1. As each layer cools and solidifies, the object gradually takes shape. One of the key advantages of FFF printing is its versatility and accessibility. FFF printers come in a wide range of sizes and configurations, making them suitable for everything from rapid prototyping in industrial settings to educational use in schools and hobbyist projects at home. Additionally, the variety of thermoplastic materials available for FFF printing allows for the creation of objects with different properties, such as strength, flexibility, and heat resistance.

However, FFF printing also has some limitations. The resolution of printed objects may be limited compared to other 3D printing technologies, resulting in visible layer lines on the surface of the final product. Additionally, certain geometries and intricate designs may be challenging to print with FFF technology, requiring support structures or post-processing to achieve the desired result. Despite these limitations, FFF printing remains a popular choice for many applications due to its affordability, ease of use, and versatility. From creating prototypes and functional parts to producing custom-designed objects and artistic creations, FFF printing continues to drive innovation and creativity in the world of additive manufacturing (Ultimaker, 2021).

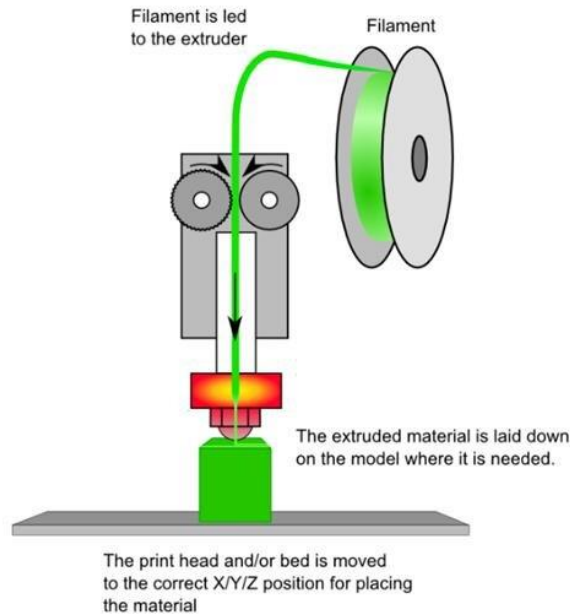


Figure 1: Schematic arrangement of the FFF process

[Source: https://www.researchgate.net/figure/FDM-processes-41-illustrates-the-FDM-process-A-plastic-filament-or-metal-wire-is_fig5_327930461]

In this project, the Ultimaker 3 extended (Appendix 2) is used because this printer has two extruders (and nozzles) resulting in the ability of printing two materials in the same layer. These extruders are situated at the back of the printer and the filament is pushed through the Bowden tubes (Figure 2) into the nozzle. Other printers use the direct drive extrusion method where the extruder is combined with the nozzle, avoiding the Bowden tubes and printing with direct communication between the extruder and the nozzle without any delay (Hullette, 2024).

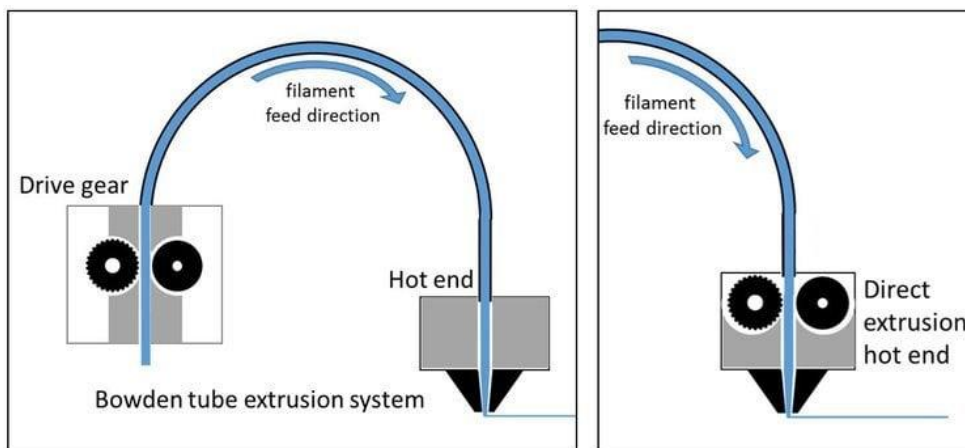


Figure 2: Extrusion systems: Bowden tubes vs direct drive

[Source: https://www.researchgate.net/figure/Left-A-Bowden-extruder-with-the-feeder-the-Bowden-tube-and-the-hotend-Right-A_fig3_335542650]

1.3 FDM applications of conductive polymers

Conductive polymers, a class of materials that exhibit both electrical conductivity and polymer properties, have garnered significant interest for their versatile applications in various fields (Ryan et al., 2022). First, primary applications are explored, followed by a focused investigation into several specific areas through in-depth investigation in chapter 3.

1.3.1 Loadcells

A load cell is a transducer used to convert force or weight into an electrical signal. It is commonly used in various industries for measuring force, tension, compression, or weight. Load cells typically consist of a metal structure with strain gauges attached. When a force is applied to the load cell, it deforms slightly, causing a change in the electrical resistance of the strain gauges. This change in resistance is then measured and converted into a readable output signal, usually in the form of voltage, current, or digital data. Using Lamé's equations, the measured strain is converted into stress to obtain the value of the applied force.

Load cells are widely utilized in applications such as industrial weighing systems, material testing machines, force monitoring in machinery, and load-bearing structures. They come in different shapes, sizes, and capacities to suit specific measurement requirements. (*What Are Load Cells and How Do They Work?*, n.d.)

Liu et al. (2021) reviewed the recent progress of 3D printed strain sensors based on different printing methods, materials, and sensing mechanisms in previous research. The results of FDM-based 3D printed strain sensors are as follows: FDM-based 3D printing is a manufacturing technique that utilizes thermoplastic polymers to fabricate strain sensors through a process involving heating-induced melting and extrusion. This method offers several advantages, including rapid printing speed, excellent strength characteristics, cost-effectiveness, and the ability to utilize a diverse array of raw materials. However, it also presents certain challenges such as surface roughness, limited interaction strength, and the relatively high melting point of the polymers used. Noteworthy examples of strain sensors produced using this technique include variations crafted from PLA, PU (Polyurethane) and, ABS (Acrylonitrile Butadiene Styrene), as well as composite materials incorporating carbon nanotubes, graphene, and other additives.

Maurizi et al. (2019) showcased the viability of employing FDM 3D-printed embedded sensors for dynamic strain assessments reaching up to 800 Hz, exhibiting a broad strain noise floor of approximately 30 $\mu\epsilon$. Additionally, it introduced a quasi-static calibration approach founded on a numerical model, corroborated by experimental findings, showcasing minimal temperature impacts and piezoresistive nonlinearities. The research underscored the constraints of these sensors at elevated frequencies, including susceptibility to electromagnetic interference, a diminished signal-to-noise ratio, and nonlinear responses. Furthermore, the study proposed prospective applications of 3D-printed piezoresistive embedded sensors within intelligent structures and systems, emphasizing their indispensable role in facilitating dynamic measurements.

After reviewing these papers, it is intriguing to consider the objective of their work in relation to the application of conductive polymer. For instance, one may aim to test the viability of the product, identify limitations, and troubleshoot issues related to using Fused Filament Fabrication for load cell manufacturing, or experiment with the application of conductive TPU. Each of these objectives presents an exciting opportunity to explore the potential of conductive polymers in practical applications and address existing challenges within the field.

1.3.2 Safety applications

For safety applications, the primary focus lays on machine safety. Large labor-intensive machines usually have safety mechanisms that prevent the machine from starting when a door is open, or a specific button is not released. Think of CNC milling machines, lathes, belt sanders, etc. A simple and inexpensive solution could be to develop a mechanism that can detect an open door, specifically a type of limit switch.

Flexible TPU could play an important role here. A hinge, of any shape and size, can be designed where a part of the hinge contains conductive material internally, which can be printed in one time. When opening and closing the door, the tension in this material will change, leading to a difference in resistance. This difference can be detected and sent to the machine's control unit so this signal can shut down the machine. In this way, existing hinges can be replaced by cheap 3D printed parts that can perform a safety function.

1.3.3 Flexible and stretchable electronics

Bilodeau et al. (2018) successfully integrated a novel, soft, stretchable central core material into their system, eliminating the need for a Joule heating wire utilized in the original design. The experiments demonstrate that actuators powered by this soft composite heater can generate comparable blocked forces while improving heat distribution through geometric optimization. Notably, a single unit of these lightweight, all-soft muscles exhibits remarkable strength, capable of lifting over 200 times its own weight. This advancement holds significant implications for the field of soft robotics, particularly in the development of autonomous systems where the ability of soft actuators to support additional weight, such as batteries and control units, is paramount.

This all-soft system represents a substantial progression from prior research, as both the soft actuator material and the soft heater hold promise for patterning via 3D printing. This approach enables automated fabrication and offers a wide array of actuator and heater shapes, while preserving the actuator's expanding performance. Although the accelerated Joule heating of the actuators renders them single use, the findings indicate repeatability at slower heating rates.

1.3.4 Antennas

Based on the experimental findings of Abdulhussein et al. (2021), the antenna parameters, including return loss (RL), voltage standing wave ratio (VSWR), gain and bandwidth, serve as crucial indicators for selecting an effective antenna, particularly tailored for S-band frequencies (frequencies between 2 and 4 GHz). The proposed antenna in that paper exhibits superior performance compared to existing references, notably in terms of RL and VSWR. The geometry of this design at the resonant frequency of 2.4 GHz is calculated with MATLAB Software. Consequently, the results from multiple performance analyses affirm the suitability of the antenna design for applications such as Wi-Fi, Bluetooth and ZigBee.

An innovative IA-based methodology was introduced to investigate the impact of fabrication tolerances on the frequency and electromagnetic (E/H) pattern of a heterogeneous 3D printed patch antenna by Wang et al. (2021). The following conclusions were drawn from this paper:

- a) In comparison to conventional numerical simulations, the proposed tolerance analysis approach effectively addresses errors associated with both the patch and the substrate, demonstrating reasonable accuracy with simplicity.
- b) The accuracy of the frequency interval is notably high when comparing simulated and tested results. While the accuracy of the E/H pattern interval is slightly lower, it remains acceptable across most angular ranges.
- c) The IA-based tolerance analysis of the frequency interval exhibits significant potential in the context of 3D printing fabrication for patch antennas. Considering that the patch serves as a primary radiation element for antenna arrays, the E/H pattern interval can also be utilized for tolerance analysis within such antenna arrays.

Fougeroux et al. (2024) introduces a novel approach to enhance the performance of planar microstrip patch antennas by leveraging FFF printing of 3D conducting patches. By incorporating pyramidal and rectangular frame extensions, the aim is to optimize antenna performance. A detailed parametric study is conducted to determine the optimal profile height necessary for achieving enhanced antenna performance. Based on the findings, the "frame shaped Electrifi antenna" with a height of 20 mm emerges as the most suitable design for experimental validation. It demonstrates a maximum gain increase of 3.4 dB, corresponding to a gain of 4.63 dBi. A similar investigation is carried out for an antenna with a copper patch material, resulting in a further 3 dB gain improvement, leading to an antenna gain of 8.1 dBi. Thus, the addition of the frame enhances both gain and bandwidth, particularly benefiting from the high conductivity of the patch material. This method effectively enhances antenna bandwidth, gain, and directivity while remaining cost-effective due to FFF 3D printing. However, there is a trade-off in compactness along the Z-axis, making it more suitable for applications with less stringent space constraints. Nonetheless, compared to a cornet-type 3D antenna, the gain/volume ratio remains superior.

Mitra et al. (2021) presents a 3D-printed microstrip patch antenna crafted from an enhanced blend of commercially available conductive Electrifi and non-conductive NinjaFlex filaments, utilizing the unique fused filament fabrication method within additive manufacturing technology. Additionally, it offers a comprehensive high-frequency characterization of the developed prototype within a fully calibrated anechoic chamber, targeting potential applications in flexible and wearable electronics across ISM bands (portions of the radio spectrum reserved internationally for industrial, scientific, and medical purposes). Employing a flexible NinjaFlex substrate, also 3D-printed, the fabricated prototype measures $65.55 \times 55.55 \times 1.2$ mm in size. Experimental results demonstrate exceptional impedance matching at a resonant frequency of 2.4 GHz and a maximum antenna gain of -2.78 dBi. These findings indicate the prototype's suitability for diverse applications such as Wi-Fi, WiMAX, and microwave satellite communications.

Striker et al. (2020) discusses an innovative manufacturing process for a single-step 3D printed conformal patch antenna utilizing two materials: Electrifi and NinjaFlex. It introduces a method to directly 3D print Electrifi and NinjaFlex together, bypassing the need for adhesives, thereby enhancing the mechanical and electromagnetic properties of the antenna. The antenna, designed for a resonant frequency of 2.32 GHz, incorporates a multi-layer stackup with a conductive ground plane and a flexible substrate. Detailed adjustments to the printing process, including temperature variations and flow rate control, ensure the production of high-quality antennas. The paper outlines the iterative process of failure analysis and improvement that led to successful antenna production, with plans to evaluate its performance in an anechoic chamber. It emphasizes the importance of precise control over the 3D printing process to achieve top-notch conformal antennas suitable for flexible applications.

The goal of the current work is to utilize a low-cost 3D printer (Ultimaker 3 Extended) to observe and address any unmentioned issues within the 3D printing process of flexible WIFI antennas. The objective also includes verifying the proper mixing of two materials, conductive (Conductive Filaflex) and non-conductive TPU (normal Filaflex). Additionally, the aim is to independently assess the performance of these materials in a real-world application.

1.3.5 Universal conducting module

A universal unit that can change in- and outputs is shown in Figure 3. When there is a fixed series of inputs and a fixed series of outputs, each input is connected to an output. When there is the possibility to put a universal and interchangeable module between those two, the same physical in- and output can be kept but it's possible to change the connections between them. This can be printed with a commercial 3D-printer which has two print cores. The idea is to print an isolated matrix with conductive lines (as connections between inputs and outputs) in different layers, so they are not connected to each other.

A field of application might be in the food processing industry. If there is a production process for a product where a component (for example, a topping) needs to change every day, it is possible to adapt it very fast with a small adjustment (changing the universal module). By being universal, the entire production process can also be modified without the need to change the physical installation.

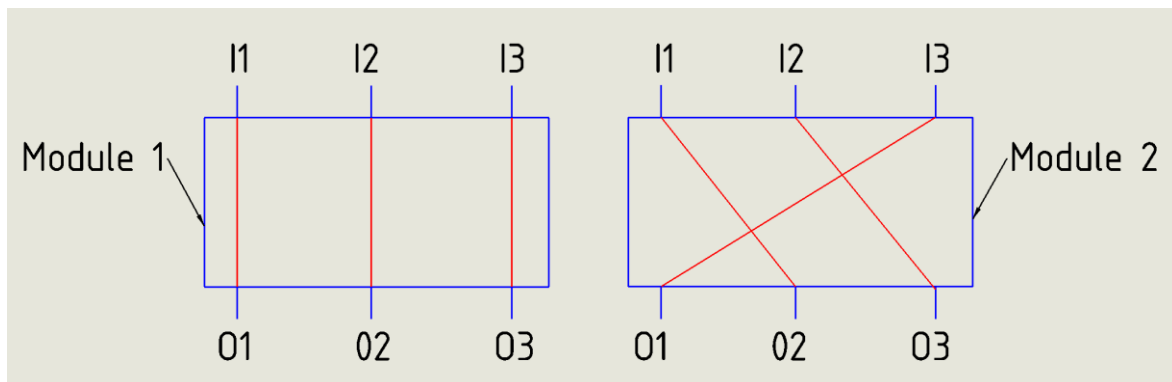


Figure 3: Universal conducting modules

1.4 Sustainable development goals

This work corresponds with several sustainable development goals (SDGs). The most relevant SDGs will be discussed in the following subsections (*THE 17 GOALS | Sustainable Development*, n.d.).

1.4.1 SDG 8: Decent work and economic growth

The advancements in 3D printing technology can lead to an economic growth through technology by creating new business opportunities in the manufacturing sector.

1.4.2 SDG 9: Industry, innovation and infrastructure

The study contributes to advancements in additive manufacturing, enhancing the capabilities and applications of 3D printing technology, particularly in electronics and sensor technology. This can be categorized as research and development.

1.4.3 SDG 12: Responsible consumption and production

This project focusses on the optimization of the use of material and the efficiency of 3D printing processes. The use of biodegradable polymers like PLA contributes to sustainable consumption and production patterns.

2 Preliminary study

In the initial test print, it is intended to determine whether it is possible to measure differences in resistance when the test specimen (Figure 5) is stretched or compressed. These results will be used later for further analysis.

2.1 Clarification test sample

To prepare the part to be printed, the Cura slicer is used. Cura is a slicing software used in 3D printing. It takes a 3D model, usually in STL (an acronym for stereolithography) format and converts, or "slices", it into instructions that the 3D printer can interpretate. These instructions include details like layer height, printing speed, temperature, infill patterns, and more (Figure 4). Cura allows users to customize various printing parameters to optimize print quality, speed, and material usage (*UltiMaker Cura*, n.d.).

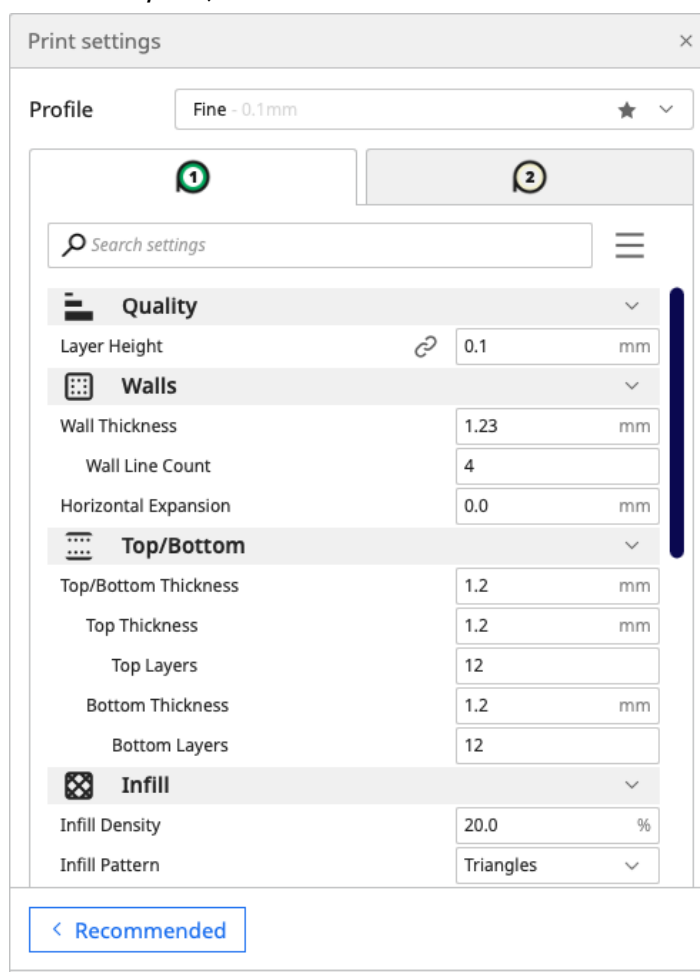


Figure 4: Example of parameters that can be modified in Cura
[Source: <https://support.makerbot.com/s/article/1667337954453>]

The total height of the specimen (and the heights in between) is a multiple of the preset layer height (0,2mm) in the Cura slicer so that the software can code each layer the same thickness. Rounding of the corners are applied to improve the print speed and quality. The conductive part itself is fully surrounded by non-conductive TPU to prevent it from external influences, only the connection points are exposed to the outside of the part and provided with tight fitting holes (2 mm) for the probes of the "MS8221A MASTECH" multimeter (Appendix 3)

2.2 Encountered problems

2.2.1 Origin orientation

A problem occurred before printing the first test. It's necessary to take the origin of each part into account while designing them. This is crucial to merge the parts correctly in the slicer (Castaneda, 2023). Later it was also found that saving the parts directly from the assembly in the CAD (Computer Aided Design) software, here SolidWorks is used, could avoid this problem.

2.2.2 "Blobby" zones

After the first test (result shown in Figure 5), some "blobby" zones were noticed at the start of each new layer. This could be solved by disabling the "retraction extra prime amount" option in the slicer. This option pushes an extra amount of material through the nozzle after the material is retracted, which is enabled at each layer hop to avoid stringing. Stringing occurs when small strings of plastic are left behind on a 3D printed model while travelling over the part without extruding material. The "blobby" zones are formed due to too much material at the start of each layer (after a layer hop).

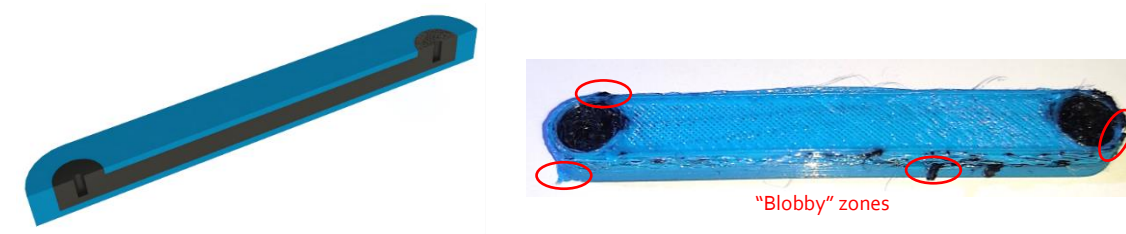


Figure 5: Test sample for test of change in conductivity.

2.2.3 Mixing problem

The overall condition of the first print was not good. It's too complicated to start immediately printing two materials in the same part. When changing the nozzle during the print, some filament was still flowing through the nozzle that was in the rest position, due to its temperature. This caused the problem that the materials started to mix while printing. This problem could be solved by increasing the retraction distance of the filament during a nozzle switch. Other problems, like very bad layer quality of the conductive filament and bad top layers occurred as well. After the first test, it was necessary to do more research on each type of filament to obtain the best settings for a qualitative print.

2.2.4 Design issue

The main design of this sample was not good for its purpose to check the difference in conductivity. Whereas all the conductive material is surrounded by non-conductive material, while bending the sample the pressure on the bottom surface was the same as the extension on the top surface what led to a zero change in conductivity.

2.3 Print parameters

As mentioned in section 2.2.3, the printing parameters of the two materials must be investigated to obtain better results in the next experiments. The Olympus SZ61 microscope is used to examine the quality of the prints and to take qualitative pictures.

2.3.1 Non-conductive TPU

Firstly, the normal (non-conductive) TPU will be examined. After initially testing the recommended print parameters (Appendix 4): standard 106% flow, 230°C nozzle temperature and speed of 45 mm/s) for this material, it was clear that insufficient material was present on the top surface, and the walls lacked attachment to the infill of the part (Figure 6 (a)).

2.3.1.1 Printing speed

This issue could be attributed to the excessive printing speed. To address this, the speed for the subsequent test was reduced from 45 mm/s to 35 mm/s. As depicted in the Figure 6 (b), this adjustment resulted in improved connectivity between the walls and infill, enhancing the quality of the top layer significantly. To further enhance the smoothness of the top layer, the print speed was further reduced to 25 mm/s (Figure 6 (c)). Despite these adjustments, some gaps persisted between the layers.

2.3.1.2 Flow rate

Consequently, in the final test, the flow rate of the extrusion was increased to 120% for the infill and 130% for the top and bottom layers, deviating from the standard value of 106%. This final adjustment yielded the optimal parameters for this material (Figure 6(d)). This conclusion is drawn based on the distance between the printed lines in the top layer. It is evident to see that in the final test, there is a good adhesion between the printed lines, resulting in a smooth surface quality. The adhesion in the infill and on the walls also contributes to a cohesive and pleasing overall appearance.

2.3.1.3 Declaration

The reason why the standard proposed parameters resulted in poor outcomes may be due to the printing method. As already mentioned in section 1.2, the Ultimaker 3 extended prints with extruders at the rear and operates with Bowden tubes. However, TPU is a challenging material to print with Bowden tubes due to its flexibility, a printer with direct drive would be more suitable. Due to the use of Bowden tubes, it is difficult for the material to be pushed through these tubes to the nozzle, and the use of retraction is very difficult to control, which can lead to under extrusion (MakeShaper, 2016).

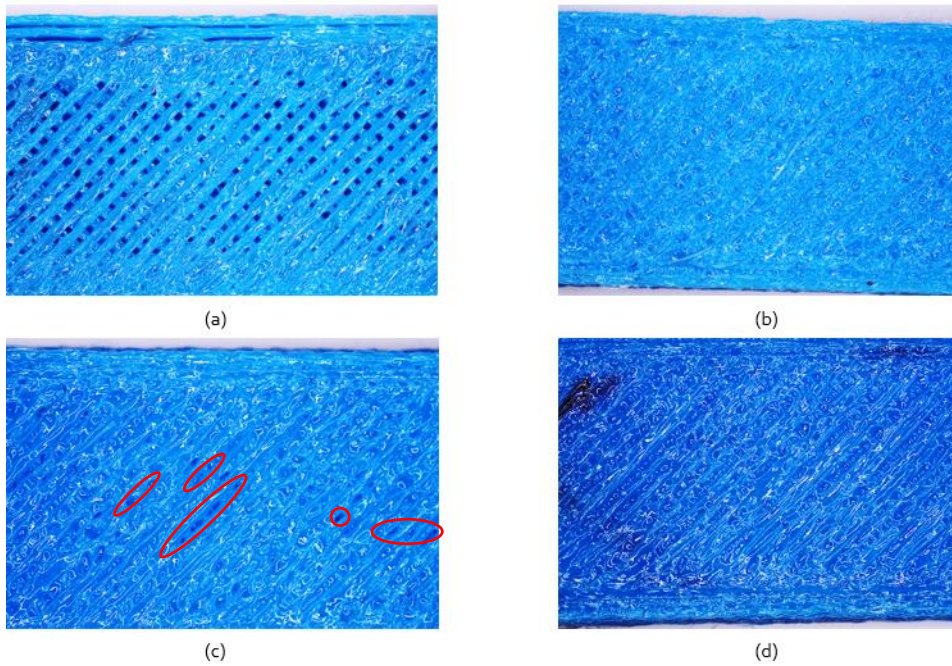


Figure 6: Test prints of not conductive material: (a) 45 mm/s (b) 35 mm/s (c) 25 mm/s and (d) 25 mm/s + 120%/130% flowrate

2.3.2 Conductive TPU

2.3.2.1 Under extrusion

For the conductive TPU, initially, the same settings used for the final result obtained with the normal TPU were applied to print the first test. The printing started well, but over time, it became messy due to insufficient material extrusion from the nozzle, indicating under extrusion. Interestingly, despite setting the flow rate to 130%, this issue persisted (Figure 8 (a)). Investigation revealed that the filament was becoming stuck in the extruder, shown in Figure 7. TPU is a soft and flexible material, if it moves too fast over too long distances through the extruder, it can bend and get stuck.

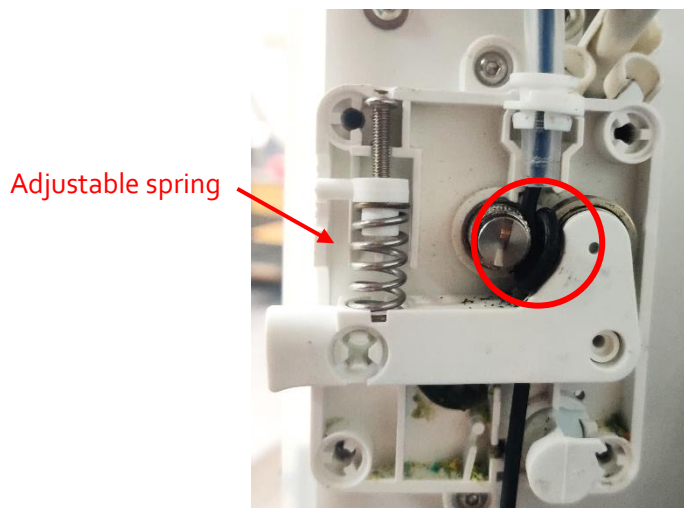


Figure 7: Obstruction in extruder

To address this, the tension of the extruder on the filament was increased by increasing the spring tension in the extruder, visible in Figure 7. However, the problem persisted, prompting a thorough cleaning of the nozzle to ensure no residual material was causing obstruction. Additionally, a higher printing temperature of 270°C was employed instead of the initial 250°C to facilitate better flow. Nevertheless, this test print also failed with the same reason: excessive pressure in the extruder. To prevent this in the next test, the pressure on the extruder was manually released each 30 seconds. At the end of the print, this resulted in a better result. It was deduced that the main issue lay in the excessive pressure within the extruder. The increased flow rate of 130%, resulting in more extrusion through the same nozzle diameter, in combination with the retraction, contributed to the rise in pressure.

2.3.2.2 Adjusted flow rate

For the next test, the same settings were retained, but the flow rate was reduced from 130% to the standard value of 106%. This alteration resulted in a better-quality print (Figure 8 (b)). This conclusion is drawn based on the overall quality of the print, determines by the distance between the lines forming one smooth surface with less imperfections.

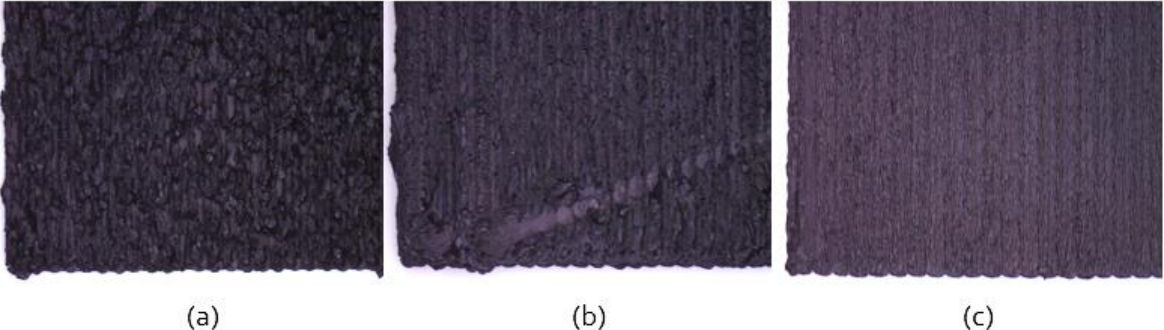


Figure 8: Test prints conductive TPU: (a) extruder pressure problems, (b) best parameters and (c) new print core

2.3.2.3 Print core failure

After multiple printing attempts, it became evident that the printer lacks consistent print quality. Print core errors (ER15 - Heater Error on Print Core, 2023) revealed issues beyond just extruder pressure, indicating a problem with the print core itself. This can have various causes: the connection of the print core with the printer, the silicone protection of the print core that maintains the temperature constant, the print parameters, Upon inspecting the print core, it was noticed that two wires responsible for communication with the printer had acquired a darker color (Figure 9). This could be related to overheating of the wires. Printing the same test sample with the same parameters using another print core, lead to a lot better results (Figure 8 (c)). It's clear to see that the line distance results in a very smooth surface without imperfections. It can be concluded that a specific design of the printer to work with TPU material is crucial to obtain good results.

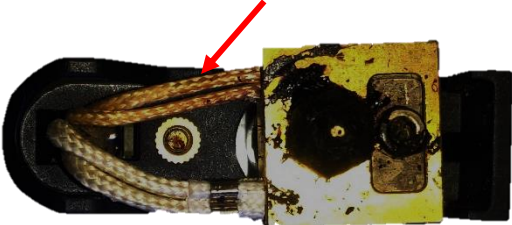


Figure 9: Print core issue, darker communication wires

2.3.3 Combination of conductive TPU with non-conductive TPU

The following step involves testing the combination of the two materials where the conductive TPU is printed in the non-conductive TPU, which acts as a pocket. While suitable outcomes were achieved with the selected parameters for each material, they will now be employed to print a part utilizing both materials. As illustrated in (Figure 10 (a)), similar results are obtained for the regular TPU (blue one), but the quality of the conductive TPU (black one) does not meet the desired excellence. One possible reason for this discrepancy could be the base material. Utilizing a glass build plate yields satisfactory print quality because of the good distribution of the heat resulting in a good material deposited over the glass. However, when the regular TPU is employed as the base, it is evident that this does not produce acceptable results because the lack of uniform distribution of the heat. The previously encountered issue of under extrusion resurfaces.

2.3.3.1 Adjustments

In the context of the second test where just one layer of the conductive TPU is printed, three critical parameters were optimized to enhance the printing process. Firstly, the nozzle printing temperature was elevated from 250°C to 260°C. Secondly, the printing speed was thoughtfully reduced from 20 mm/s to 15 mm/s. Lastly, the system was fine-tuned by increasing the flowrate to 110%. Notably, this adjustment, which had previously caused problems, resulted in significantly improved outcomes during the second test (Figure 10 (b)).

For the third and final test, only the speed and flow were adjusted. The speed was reduced to 12 mm/s, and the flow was increased to 115%. With these settings, a good result is obtained that can be used for further applications (Figure 10 (c)).

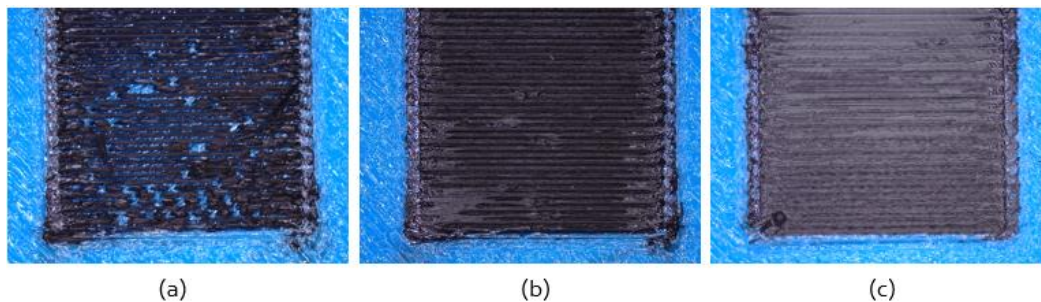
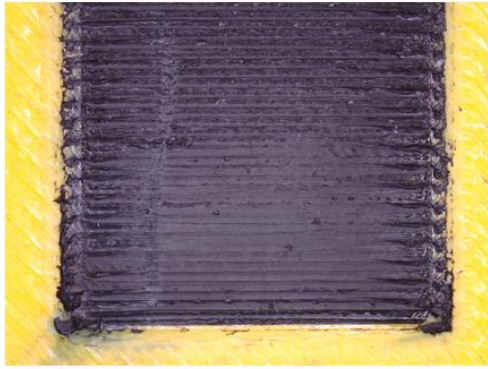


Figure 10: Experiments combining materials: (a) previously determined settings, (b) reduced speed, increased heat and flow, (c) further increased flow and decreased speed

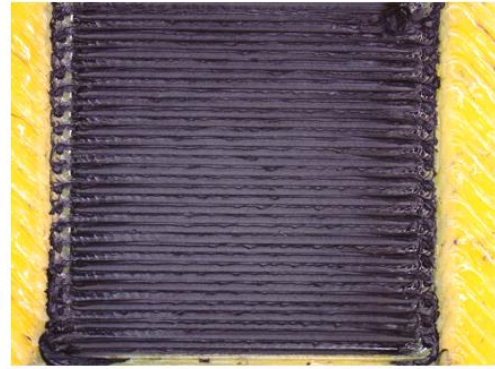
2.3.4 Combination of conductive TPU with PLA

Following successful results achieved using a blend of normal TPU and conductive TPU, the subsequent phase involves conducting tests on the part while substituting the normal TPU material with PLA. This aims to explore the feasibility of combining the conductive one with another material of different nature. The first test led to good results and an acceptable sample (Figure 11 (a)).

It is noticeable that the beginning of the conductive TPU layer has a lesser amount of material compared to its end. This discrepancy was observed in previous tests as well. Adjusting the "Nozzle Switch Extra Prime Amount" setting to 0,8 mm³ could potentially address this issue. This value was set to zero in section 2.2.2 to prevent the "blobby" zones but was only necessary for the non-conductive material. When this option is enabled, the extruder pushes an extra amount of material through the nozzle after a nozzle switch. Figure 11 (b) shows that this setting results in an evenly spread layer quality but there is a small overlap between the lines. The higher viscosity resulting from the elevated printing temperature can explain this. To mitigate this, the distance between the lines will be enlarged from 0.4 mm to 0.6 mm in the next test (Figure 12 (a)). This adjustment results in a gap between the lines so this value is adjusted to 0,5mm (Figure 12 (b)) which is a value that can be used in the next tests.



(a)

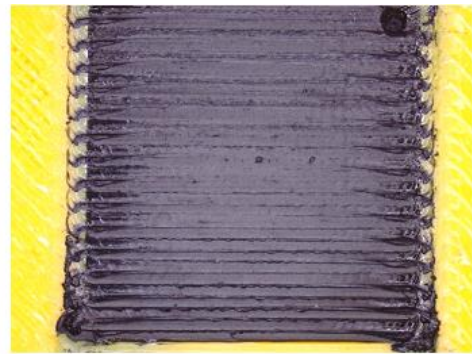


(b)

Figure 11: Combination conductive TPU with PLA: (a) parameters and (b) with "Nozzle Switch Extra Prime Amount" setting on



(a)



(b)

Figure 12: (a) line distance 0,6 mm and (b) line distance 0,5 mm

3 Chosen applications

In this section, three applications are examined in more detail: the circuit board, the load cell, and the antenna. The selection of these applications is based on previously acquired information from the literature study. It can be concluded from this information that these applications are feasible to produce with a discussable outcome.

3.1 Circuit board

The purpose of this experiment is to print a simple circuit board that can be used for basic applications.

3.1.1 Design and methodology

In this setup (Figure 13 (a)), an adapter type PA-1900-05 (Appendix 5) is connected to the power grid, which converts a mains voltage of 230 AC volts to 19 DC volts. In the circuit, this voltage will be converted via a transistor type L7805CV (Appendix 6) to a voltage of 5 volts. The objective is to measure a constant voltage of 5 volts as the output of the transistor. The combination of the LED light in series with a resistor, is connected in parallel with the output to verify its operation (Figure 13 (b)).

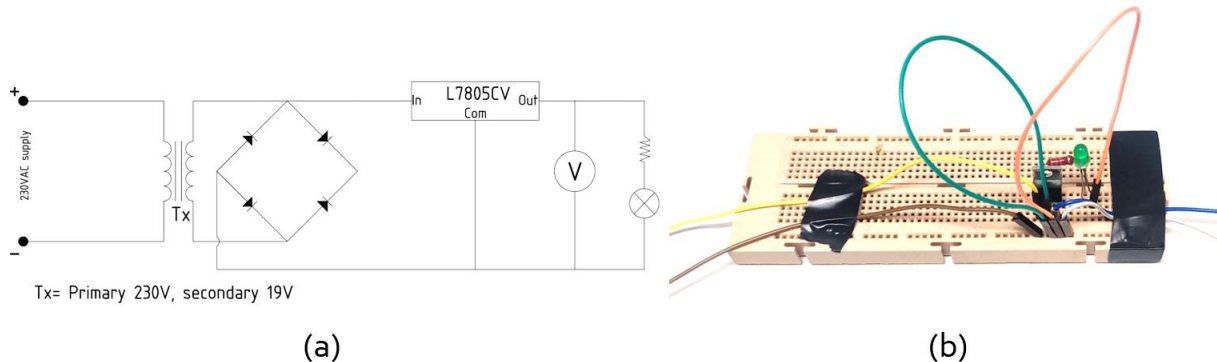


Figure 13: (a) Electrical diagram and (b) Experimental setup on breadboard

3.1.2 Problems and results

Based on 2.3, the design (Figure 14) was printed with the best fitting print parameters. The infill type of the conductive part, TPU conductive, is adjusted to lines where all the lines are printed in the same horizontal direction (way of current flow) to obtain the best conductivity. To make the connections between the printed circuit and the hardware components, a soldering iron for electronic components is used. PLA is used to embed and protect the conductive printed lines. In a normal circuit board, the circuit's conductive tracks are completely accessible, only protected with a layer of varnish to avoid oxidation, in some cases. Due to the non-conductive nature of the initial layer, establishing a reliable solder connection becomes challenging (Figure 14 (b)). To prevent this, the design is modified to ensure the conductive part initiates within the first layer. However, an issue arose during the printing of this sample: certain unions were formed between the hardware's connection points. Consequently, this lack of isolation among the various feed lines led to a short-circuit problem (Figure 14 (c)).

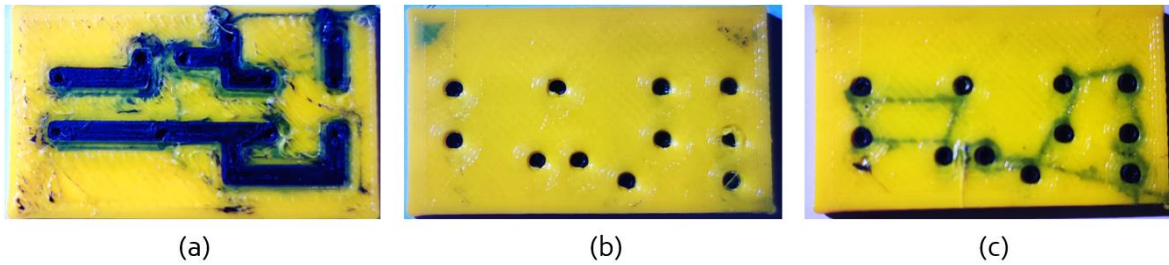


Figure 14: (a) Top view, (b) Non-conductive bottom layer and (c) bottom layer with conductive connections

The decision was made to reprint the initial design while soldering the hardware components onto the top side (Figure 14 (a)) of the part rather than the bottom. This side offers significantly more conductive material, enhancing the ability to achieve a strong solder connection. This resulted in good connections.

With a good-composed circuit board, some measurements could be made. The adapter has an output of 19 volts, but when measuring at the transistor's input, only 16 volts is detected. This indicates that some hardware connections are subpar. An adapter piece was used to make it easy to replace the transistor when it fails or in need of another one (Figure 15 (a)). It was noticeable that when the transistor was plugged in to this adapter part, the voltage dropped approximately 3 volts. To prevent this, the transistor is soldered directly into the circuit board (Figure 15 (b)). These connections were resoldered to ensure optimal connectivity, resolving the voltage drop upon re-measurement.

Even though a stable 4.93 volts is measured as the output of the transistor, the LED light is not bright enough. This implicates that the resistance in the circuit is too high. When reducing the external resistor of 2 kilo ohms to 200 ohms, the problem is partially solved. It can be declared, after measurement, that the resistivity of the conductive TPU is causing this behavior. The voltage is kept constant, but the intensity decreases because of the increased resistance. It is an important behavior to take into account when a conductive TPU is used as a circuit's track.

To conclude this sub research, it is evident to say that good solder connections are necessary to obtain good results. Further research could be done with conductive PLA or another nonflexible conductive material. This can result in options to print feeding lines in different layers. This is almost impossible with flexible material, as conductive TPU, due to its stringing problem which leads to connections between the different feeding lines causing short-circuit.



Figure 15: (a) with adapter piece and (b) without adapter piece, final result

3.2 Strain Gauge

In this section, the possibility of printing strain gauges using conductive filament, as previously mentioned in 1.3.1, is investigated.

3.2.1 Methodology

The objective is to measure a change in resistance when the sample is stretched or compressed. By applying tension to the test piece, the cross-section will narrow or widen, making it more difficult or easier for electrons to move through the material resulting in a change of resistivity.

To measure this difference, a voltage divider (Braza, 2020) is used, using an Arduino setup (Figure 16). Since the absolute resistance changes of the 3D-printed strain gauges are much greater (Ω instead of $\mu\Omega$) than the classic ones, the voltage divider was chosen instead of other circuits such as the Wheatstone Bridge (*Wheatstone Bridge Circuit | Strain Gauge*, n.d.) to measure the change in resistance. Based on the voltage divider formula (equation (1)) where R_2 is a known resistance, V_s is the known input voltage of the Arduino UNO R_3 (*UNO R3 | Arduino Documentation*, n.d.) and V_{R_2} is read from the analog pin of the Arduino, an unknown resistance R_1 can be determined by calculating the voltage drop over the second resistor. R_1 will represent the strain gauge.

$$V_{R_2} = V_s \cdot \left(\frac{R_2}{R_1 + R_2} \right) \Rightarrow R_1 = R_2 \cdot \frac{(V_s - V_{R_2})}{V_{R_2}} \quad (1)$$

To visualize these results, a combination of code is written in Arduino and MATLAB (Appendix 7 and Appendix 8) to plot the resistance in function of time. A short pause is added to the end of the loop to filter the deviations due to vibrations and other external effects. This is also necessary to give the computer's CPU some time to calculate, otherwise it will overload.

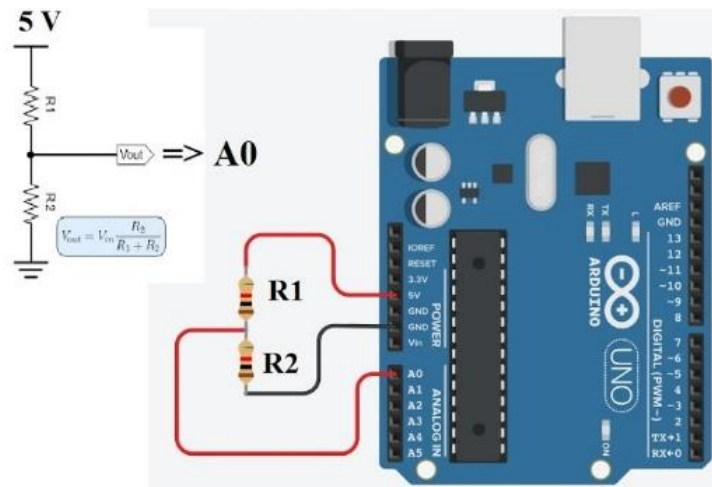


Figure 16: Voltage divider Arduino setup
[Source: https://www.youtube.com/watch?v=7XvHye7bx_o]

3.2.2 Arduino setup test

Firstly, the code is tested with R_1 as a known variable resistor with a range between 0 and 5000 ohms. While running the code, the resistance of the variable resistor is manually changed a couple of times to check whether the change in resistance on the graph is accurate to draw some conclusions. As shown in Figure 17, the quality of the graph is good to use for further investigation. Some deviations are visible at certain points in the graph, these depend on the duration of the measurement and the quality of the connections in the circuit. When using this setup in further investigation, this can be finetuned by adjusting the pause at the end of each loop.

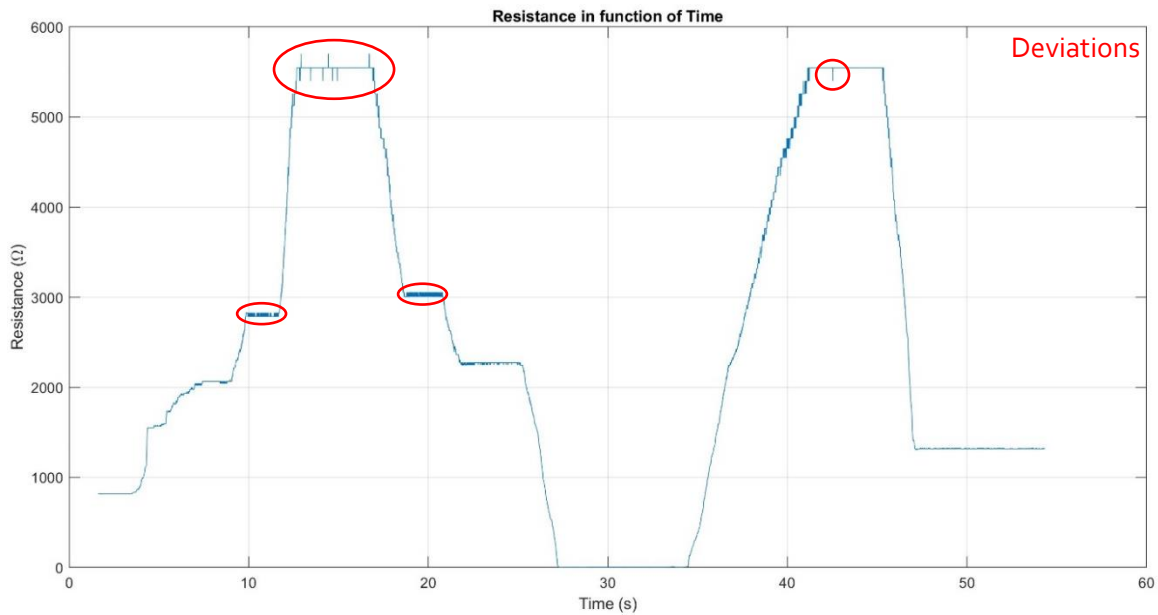


Figure 17: Resistance in function of time using a variable resistor

3.2.3 Design of sample

The design (Figure 19) of the test sample is based on a standard linear strain gauge (Figure 18) and consist of a two-layer base of TPU with on top one layer of conductive TPU.

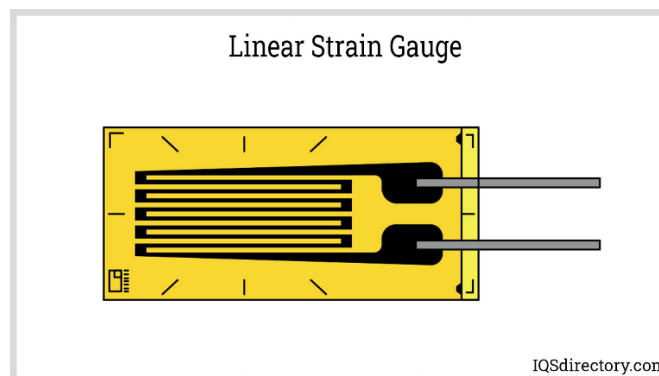


Figure 18: Model of a standard linear strain gauge
 [Source: <https://www.iqsdirectory.com/articles/load-cell/strain-gauge.html>]

The conductive part (horizontal lines) is designed in SolidWorks as a rectangle shape. The infill options in Cura are used to obtain different lines next to each other. To get the wanted design, the line width is adjusted to 0.7 mm instead of the standard value of 0.4 mm combined with a line separation of 2 mm, the infill pattern is set to "Zigzag", and the wall count is set to a value of zero, to remove the outside connections. With these settings, the designed rectangle is sliced into the model of a strain gauge. Two extra rectangle shapes are added to the part to make a good surface to connect the needed wires. To avoid that Cura slices these parts the same way as the conductive lines, the option "per model settings" is used. With this option enabled, it's possible to adjust the settings of each different part in the design printed by the same nozzle. Here, the line distance of 2 mm is overwritten by an infill of 100% and the wall count is set to the value of 1.

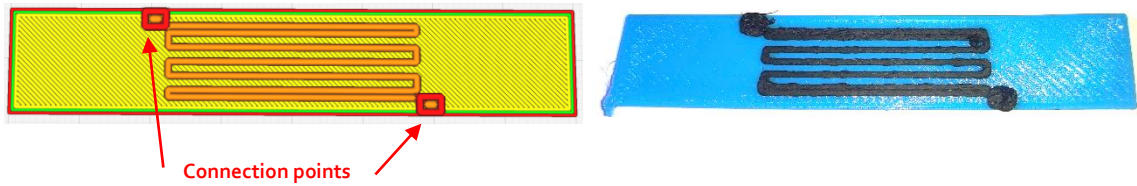


Figure 19: Design of strain gauge

3.2.4 Pretesting the samples

The design (sample 1) resulted in a good quality print because a constant resistance could be measured with a multimeter, approximately 270 k Ω . Trying to connect the sample to the Arduino setup led to the calculation of an infinity resistance value. The reason for this is that the internal resistance of the lines in the sample is too high causing a very low voltage drop that couldn't be measured with the analog pin of the Arduino. To increase this voltage drop, the resistance in the conductive lines must be decreased. To obtain this, the one-layer conductive material is adjusted to three layers, resulting in resistance of approximately 40 k Ω . This value could be measured by the Arduino making this sample suitable for the next step.

After printing several test pieces, it was noticeable that the resistance in the strain gauge was not consistent although it was printed with the same settings. Small connections between the conductive lines were noticeable. (Figure 20). These connections are not the same on each part, causing a different resistance. After manually removing these connections, still some difference in resistance was measured.

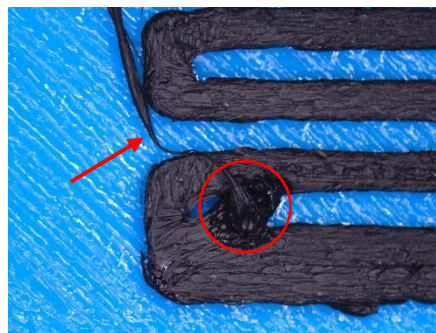


Figure 20: Connections between conductive lines

Doing some research on the material itself led to the conclusion that the conductive TPU wasn't conductive overall. When connecting the probes of the multimeter to the cylindrical part of the filament, a resistance was measured. While measuring on the cross section of the material (after cutting it), no resistance was detected. Based on this, a conclusion can be drawn that the material is covered with a conductive coating instead of using the production process described in 1.1. This alternative way of production is used to keep the flexibility of the material whereas the additives, which are usually stiff and brittle, limit this material property (Grellmann et al., 2021). When the material is melted in the nozzle of the 3D-printer, the TPU is mixed with the conductive coating making the extruded material conductive. This principle can lead to inconsistent conductivity by reprinting the same part with the same settings. The retraction of the material can disturb the mixing process. For this reason, it is not suitable to use this design for 3D printed strain gauges with this material. Because of the inconsistency of the conductivity, the calibration of the parts would not be the same. Another explanation why the material did not have a consistent conductivity is the extruder problem explained in section 2.3.2.1. Due to the high pressure in the extruder, the extruder wheels can damage the conductive coating resulting in less conductive particles mixing in the nozzle.

To proceed with the test, a new design (sample 2) was created: a basic rectangle consisting of two layers of conductive TPU. This sample is placed (Figure 21(b)) in the INSTRON 5967 (5900 Series Universal Testing Systems, n.d.) to test the variance of resistivity when extended. The first sample is also tested in this machine (Figure 21 (a)).

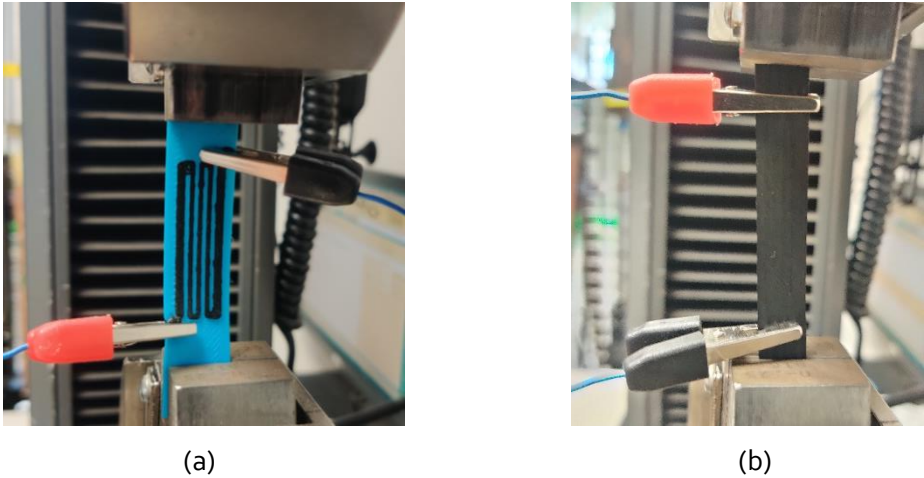


Figure 21: Sample 1 (a) and sample 2 (b) in Instron machine

3.2.5 Results

As shown in Figure 22, there is too much variation in the data to take some conclusions. A reasonable explanation for this is the connection between the sample and the Arduino setup. A set of crocodile clips are placed on the sample at the designated location. This not consistent connection can lead to this variation in data.

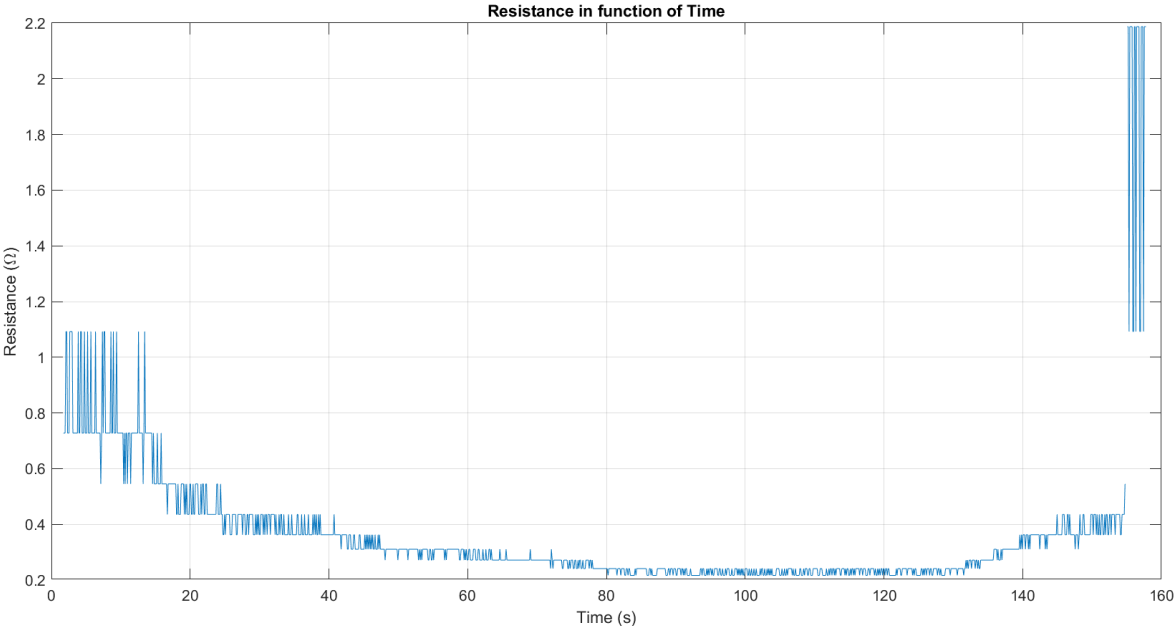


Figure 22: Resistance in function of time sample 1

When a normal strain gauge is stretched, its conductors elongate and become thinner, leading to increased resistance. Conversely, when a strain gauge is compressed, its conductors shorten and widen, resulting in decreased resistance (Staff, 2020).

Figure 23 is created by plotting the change in resistance measured with the Arduino as a function of the extension measured by the Instron machine at the same associated time value. As shown in this figure, the resistance decreases when the sample is stretched. This is an opposite operation

compared to a standard strain gauge. This could be justified by the properties of the material. When stretching, the connections between the printed lines and layers form a more consistent whole, resulting in a better conductivity. Another related influence is that the conductive particles inside the material perform better (they stay more stuck) when they are under tension. It is noticeable that the resistance increases near the end. This can be declared by the high tension between the lines resulting in losing connections, creating holes. It can be concluded that there is a non-linear inverse proportional relation between the extension and the resistance of the material.

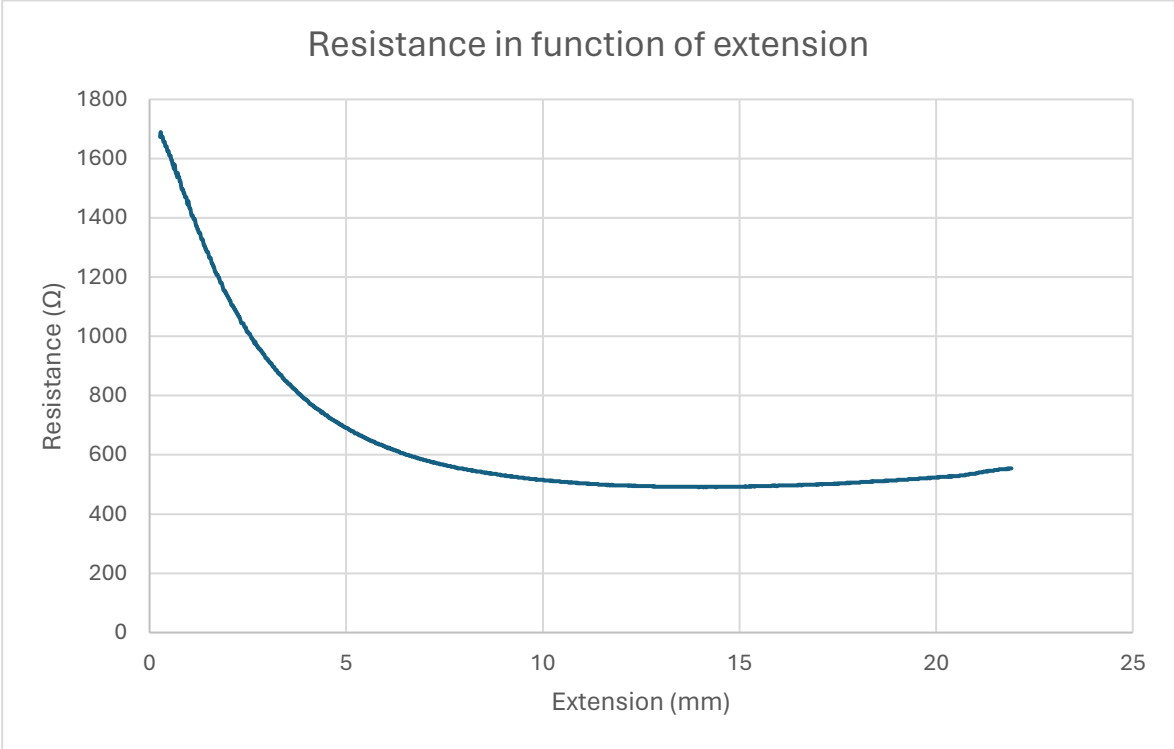


Figure 23: Graph of resistance in function of extension sample 2

3.3 Antenna

In this section, the possibility of printing patch antennas using conductive filament, as previously mentioned in 1.3.1, and the operating problems are investigated.

3.3.1 Design

The patch of the antenna is designed and simulated in Ansys HFSS (Striker et al., 2020) and optimized for a resonant frequency of 2.32 GHz which is close to Wi-Fi network of 2.40 GHz that will be tested. The stack up (based on the findings of Striker et al. (2020)) consists of a 0.2 mm conductive TPU ground layer, a 1.2 mm non-conductive TPU substrate and a 0.2 mm conductive TPU patch layer on top. This design is showed in Figure 24.

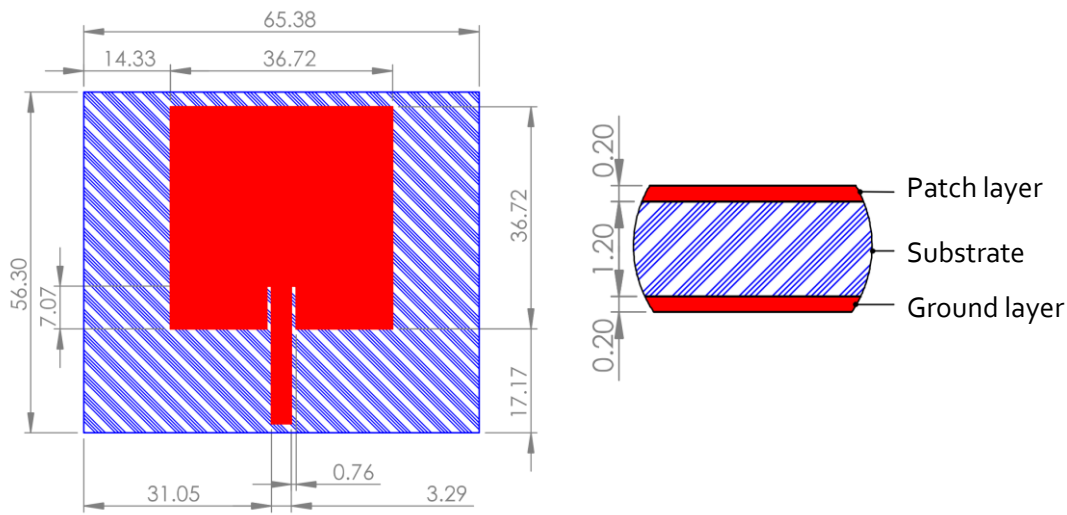


Figure 24: Patch antenna design and dimensions in millimeters (Striker et al., 2020)

3.3.2 Printing of the antenna

For printing the design, the print parameters obtained in section 2.3.2 are used. The first print (Figure 25 (a)) led to insufficient material in the patch layer. This was caused by an obstruction in the extruder which already happened in section 2.3.2.1. The fact that this phenomenon happened again is due to the printing duration. In the previous tests and applications, the printing time of the conductive TPU was short because of the small samples. This sample is bigger, increasing the printing time.

The known problem of the obstruction in the extruder is caused by a too high pressure. By regulating the flow, this problem was temporarily gone. When printing larger pieces, the pressure in the extruder builds up. That's why the first layer (also in conductive TPU) has a good quality but after time, the pressure becomes too high causing an obstructing in the extruder resulting in a failed patch layer.

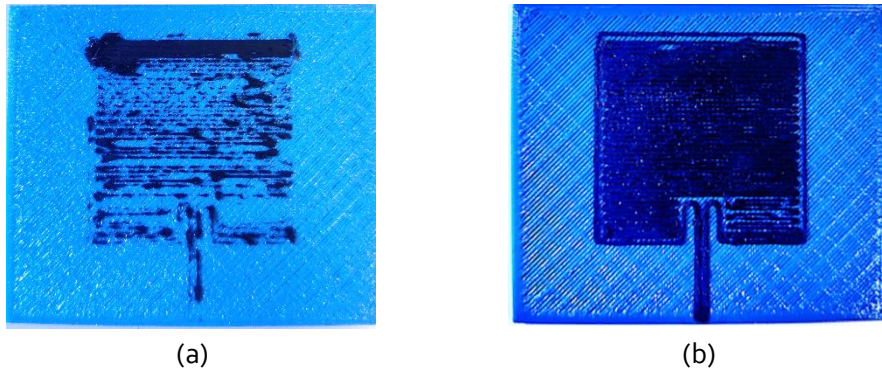


Figure 25: Test one (a) and two (b) of printing the antenna

The second test (Figure 25 (b)) resulted in a better quality of the top layer (more homogeneous material) because the flow in the patch layer was reduced using the “per model setting” in the Cura slicer, reducing the pressure in the extruder. With this setting, it’s possible to change parameters for each part of the print separately. Still, not enough material was present in the patch layer. By increasing the standby temperature of print core two (with the conductive material) from 125 °C to 180°C, a much better result was obtained. Enough material was spread over the patch layer, only some gaps between the lines and walls are noticeable. The reason why this setting improves the quality, is because at a too low standby temperature, impurities (not fully melted material, dust, or the combination of both) can cause obstructions in the nozzle. After an iteration of testing with the following settings:

- **Infill line width:** affecting the width of all the lines in the infill of the layer.
- **Infill overlap:** affecting the overlap between the infill lines and the wall lines.
- **Wall flow:** affecting the amount of material pressed through the nozzle while printing the wall lines.
- **Wall line width:** affecting the width of all the wall lines in the infill of the layer.

the result shown in Figure 26 was obtained. An overall good quality print with sufficiently spread material over the layer. It is still noticeable that there are small gaps between the inner- and outer walls.

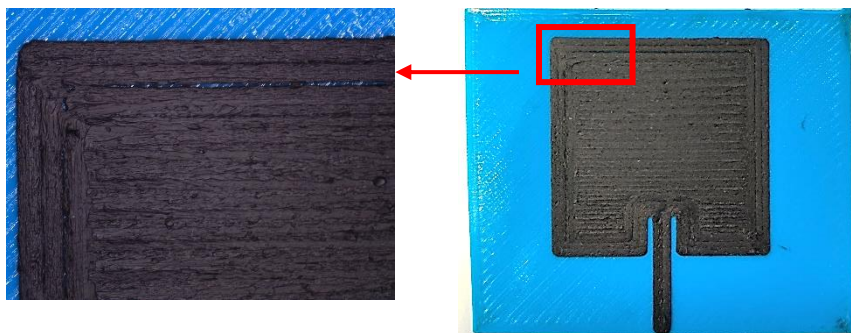


Figure 26: Result after iteration of parameters

To smoothen the surface into a consistent whole without gaps, the ironing setting on the top layer is enabled (Cura, 2024). This setting adds an extra step to the end of the printing process. With this setting enabled, the hot nozzle wipes over the top of the print while extruding a very small amount of material, trying to connect all the gaps while smoothening the surface.

As shown in Figure 27 (a), the ironing feature did not lead to the wanted result. The gaps in the top left corner increased in size. It is noticeable at the start point of the ironing process (bottom right corner), that way too much material is spread. Also, other parts of the antenna marked in Figure 27 (a) have a bad quality due to bad material spread. This conductive TPU is too sensitive to use the ironing feature, because of its flexibility and difficult behavior for example: retraction issues, stickiness, and it cools quickly.

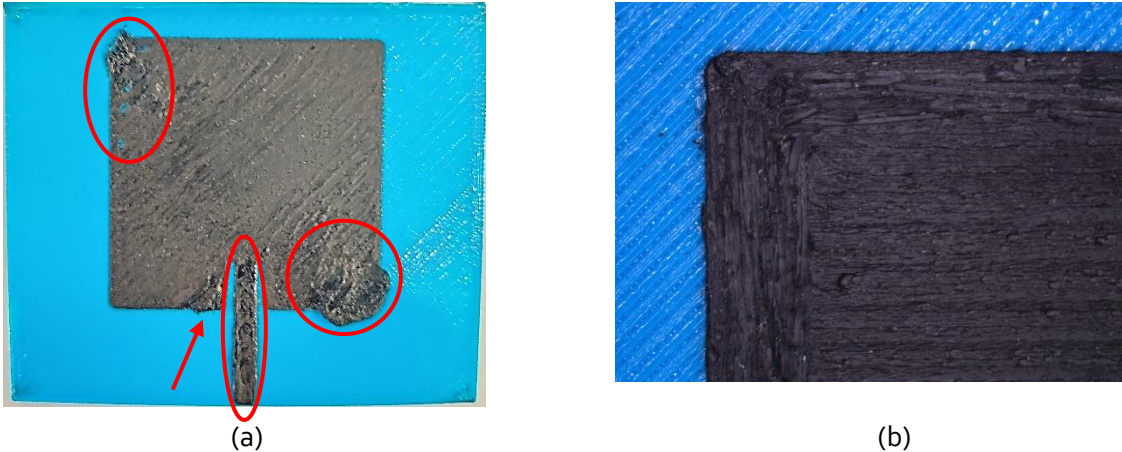


Figure 27: (a) Result after ironing (b) Results after manual manipulation

To obtain the best sample, the best possible combination of settings gained in the iteration process, showed in Figure 26, is manually manipulated. A soldering iron is used to connect to gaps between the wall lines, in combination with a piece of filament as additive. This last result is shown in Figure 27 (b) and used for further investigation of the behavior of the antenna. Therefore a SMA-RP connector is attached to the antenna as shown in Figure 28.

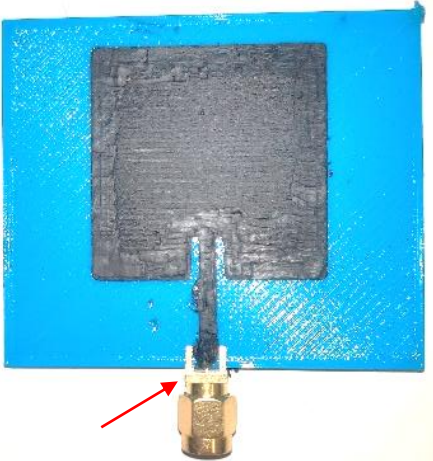


Figure 28: SMA-RP connector on antenna

3.3.3 Methodology

To evaluate the performance of the antenna, the emitting and receiving behavior of the antenna are tested.

3.3.3.1 Working principle of an antenna

An antenna acts as a transducer, converting electric current into electromagnetic (EM) waves and vice versa. It can transmit EM waves when connected to a transmitter and receive EM waves to generate electric current for a receiver. The design of an antenna is influenced by its intended frequency, direction, and signal strength (*What Are Antennas and How Do They Work?*, n.d.).

3.3.3.2 Return loss

In practical applications, the S_{11} parameter is frequently referenced when discussing antennas. S_{11} indicates the amount of power reflected from the antenna, known as the reflection coefficient or return loss (RL). It represents the ratio of radio waves received at the antenna input that are refused to those that are accepted (equation (2)), specified in decibels (dB). Generally, a lower (more negative) return loss value is preferable where more power is accepted and radiated by the antenna and less is reflected. The Voltage Standing Wave Ratio (VSWR), a dimensionless ratio, indicating the same parameter as return loss but on a different scale (equation (3)). It represents the maximum and minimum voltage level along the entire length of the transmission. (*S-Parameters for Antennas* (S_{11} , S_{12} , ...), n.d.)

$$RL \text{ (dB)} = 10 \log_{10} \frac{P_i}{P_r} \quad (2)$$

$$VSWR = \frac{1 + \sqrt{P_r/P_i}}{1 - \sqrt{P_r/P_i}} \quad (3)$$

With P_i the incident power and P_r the transmitted power

The common return loss values are compared in Table 1 (Bureau, 2023).

Return Loss	What It Means	VSWR Number
-0 dB	100% reflection, no power into the antenna, all reflected back	Infinite
-1 dB	80% reflection, 20% power into the antenna	17
-2 dB	63% reflection, 37% power into the antenna	9
-3 dB	50% reflection, 50% power into the antenna	6
-5 dB	32% reflection, 68% power into the antenna	3.5
-6 dB	25% reflection, 75% power into the antenna	3
-8 dB	16% reflection, 84% power into the antenna	2.3
-10 dB	10 dB (10% reflection, 90% power into the antenna)	2
-15 dB	15 dB (3% reflection, 97% power into the antenna)	1.4
-20 dB	20 dB (1% reflection, 99% power into the antenna)	1.2

Table 1: Relation Between Return Loss, Power % Reflected Back and VSWR

3.3.3.3 Reception

To assess the reception strength of the antenna, the campus network, namely UPVNET, is utilized. Using a Wi-Fi monitoring application, the signal strength of the network is initially determined without the antenna. Subsequently, the antenna is connected to the computer using a Wi-Fi USB antenna adapter, and the signal is tested again. The purpose of this setup is to observe an amplification of the signal.

3.3.4 Results

3.3.4.1 S₁₁ factor (return loss)

The S₁₁ parameter is examined using a Vector Network Analyzer (VNA), shown in Figure 29. With the VNA, the antenna's behavior is evaluated, it does not differentiate between emission and reception. Before extracting the data from the VNA, the machine needs to be calibrated. The connection cable and adapter parts have a negative influence on the measured return loss. When the machine is calibrated, this influence is included in the result. When measuring the radio frequency (RF) of the antenna, it was noticed that there was a return loss more than zero decibels, resulting in all the power being reflected. Further investigation and iteration of the frequency range led to better results. At the frequency of 1.53 GHz, a return loss of -13,47 dB is measured (Figure 30). This corresponds to a value between 90% and 97% that is powered into the antenna according to Table 1. It can be declared that the printed antenna can be used to transmit and receive signals and thus this material can be processed in applications without the need for an external antenna.



Figure 29: Antenna connected to VNA

As mentioned in section 3.3.1, the design is made for a frequency of 2.32GHz but at that frequency the radio waves are only reflected. The dimensions of the part and the dielectric behavior of the non-conductive TPU between the patch and the ground layer, define the best operating frequency (Striker et al., 2020). Because the dielectric material is not the same as in the prementioned study and the patch is manipulated to close the gaps, the change in operating frequency can be justified. The connection of the SMA connector piece can influence the transmitting of the signal causing a change in operating frequency. The resonant frequency of the antenna can be modified by modifying its dimensions to adapt them to the peculiarity of 3D printing and thus obtaining the target frequency.

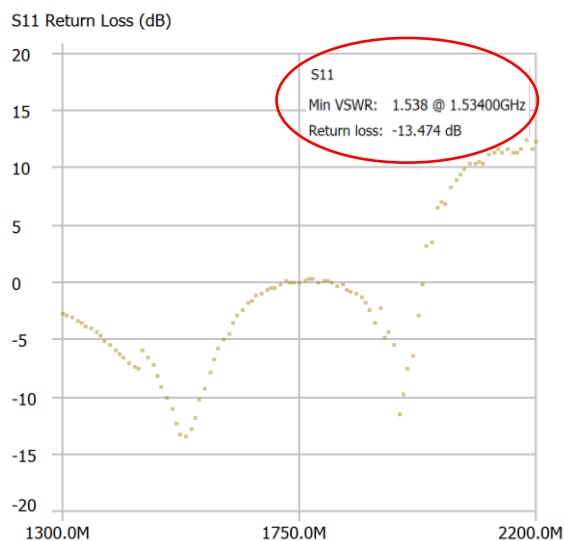


Figure 30: Measured return loss

3.3.4.2 Antenna reception test

The measurement is started by measuring the signal strength of the computer's internal receiver. During the measurement, it switches to a measurement using the USB adapter. Only the top blue signal is investigated, the other signals are other available WIFI networks. The moment where the switch happens is visible in Figure 31 where the signal strength weakens (a loss of about 9 dBm). The overall performance of the antenna is certainly sufficient to receive a Wi-Fi network but results in a weaker signal than the reception of the internal receiver. Based on this test, it can be concluded that printing an antenna is certainly an interesting application to receive signals, but not to outperform a particular (standard) receiver.

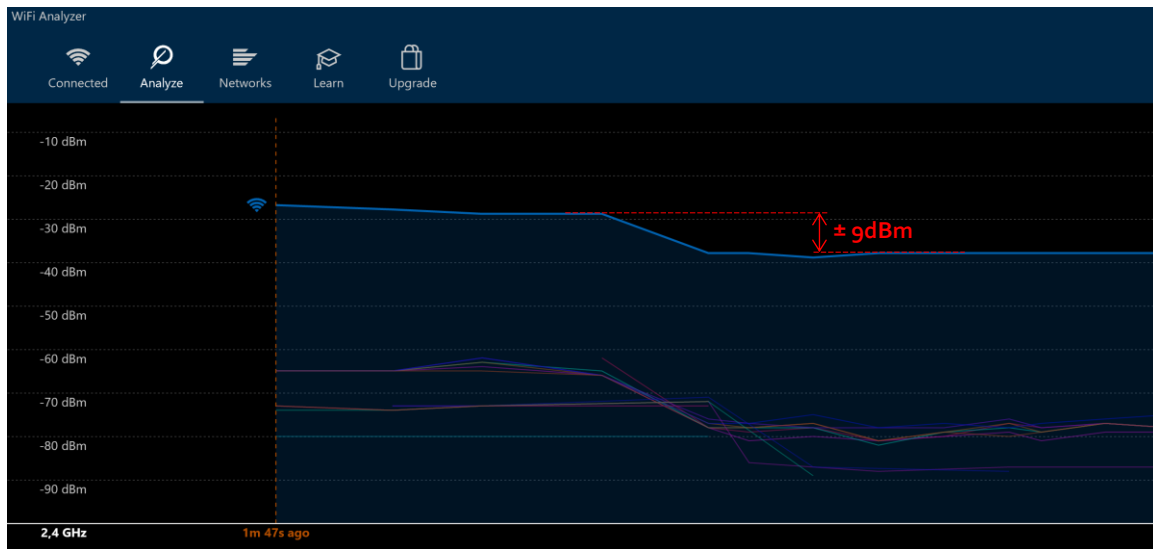


Figure 31: Comparison internal receiver vs printed antenna

4 Material behavior

As mentioned in section 3.2.4 the conductive behavior of the material is not consistent. In this section, this behavior is investigated. Since the conductive graphene coating is mixed with the filament in the nozzle, this aspect of the printing process needs to be examined. To improve the mixing process, some parameters (Table 2) effecting this mixing process are tested. Firstly, the distance between the lines is investigated. When the lines are closer to each other, there is an extra mixture of the material between different printed lines. The second parameter is the layer direction, causing longer or shorter overlaps between two lines. The temperature, which is an important parameter, is kept constant at 250 °C. With this value, the best results have been obtained in previous sections.

	Sample 1	Sample 2	Sample 3
Line direction	[90] (horizontal)	[0] (vertical)	[90] (horizontal)
Line separation	1 mm	1 mm	0,8 mm
Temperature	250°C	250°C	250°C

Table 2: Print parameters samples

4.1 Methodology

To test these parameters, a three-layer basic rectangular shape (40 x 10 x 0,6 mm) is printed. The measured distance between the probes of the multimeter must be the same for each sample. Therefore, a caliper is used to mark the measuring points on the samples with a separation of 20 mm. The test pieces are also given some time to cool down after printing, ensuring measurements are taken at consistent room temperature.

4.2 Results

4.2.1 Decreasing resistance

When measuring the resistance of the material, it was noticeable that the resistance was decreasing during the measurement procedure. To analyze this phenomenon, a sample is connected to the Arduino setup used in 3.2. As shown in Figure 32, it's clear that after some time the resistance is decreasing while taking measurements and stabilizes after approximately five minutes.

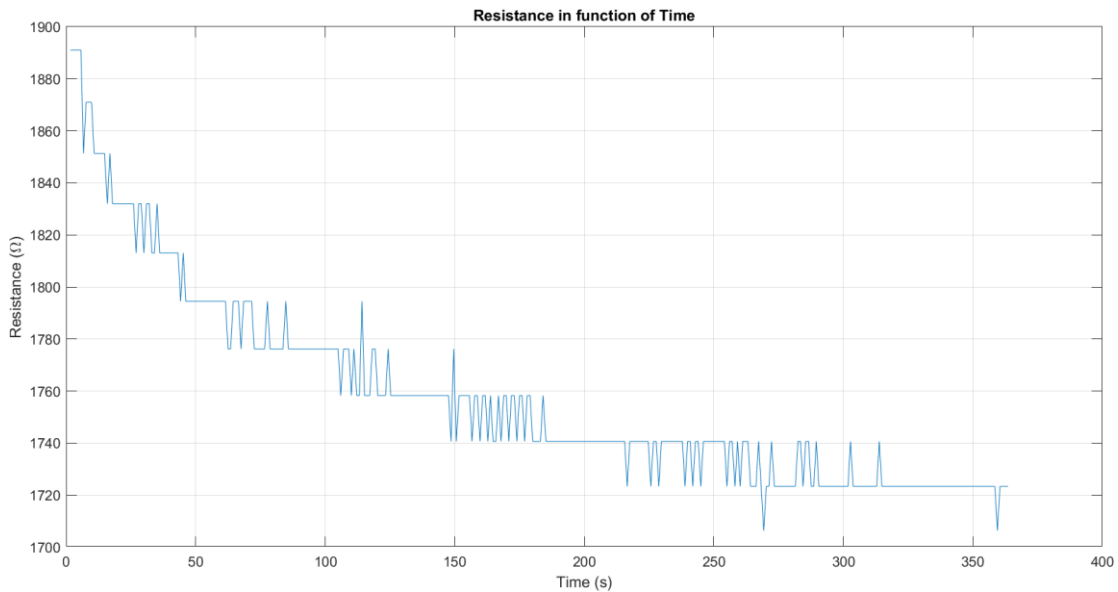


Figure 32: Decreasing resistance in function of time

This phenomenon could be explained by the fact that the conductive particles in the material start to arrange themselves in a more organized manner when a low current flows through. As a result, electrons can move more smoothly through the material, thus demonstrating lower resistance. This is an assumption made to interpret the graph, but it cannot be explained with certainty.

4.2.2 Consistency

The goal of this experiment is to check if the resistance is consistent when printing the same samples three times (A, B and C in Table 3) with the same parameters, specified in Table 2, adjusting only one parameter between the different samples. Because of the phenomenon mentioned in section 4.2.1, the probes are placed on the sample and the value of the resistance is captured after timing 10 seconds.

	Sample 1	Sample 2	Sample 3
A	2,83 kΩ	2,58 kΩ	2,74 kΩ
B	1,87 kΩ	2,08 kΩ	2,62 kΩ
C	1,39 kΩ	2,82 kΩ	2,76 kΩ

Table 3: Results of consistency test

Based on the results (Table 3), the direction of the lines doesn't lead to a consistent resistivity. The line separation of sample three which is less than the line separation of sample one, leads to a more consistent result. This could be explained by the fact that there is more mixture between the different lines due to more overlap, making the material more equal distributed.

4.2.3 Extra investigation on retraction

The samples in 4.2 were printed one by one so no retraction was enabled. In section 3.2.4, the samples were printed using different nozzles, enabling the retraction option when changing them. When the material is retracted at a change of nozzle, some melted material is pulled out of the nozzle. When printing again with this nozzle, the material is pushed again in the direction of the nozzle. This event could have an impact on the mixing process so is investigated in this subsection.

4.2.3.1 Methodology

For this test, two samples with different retraction distances are created and measured with the same method as in section 4.2.2. The other fixed parameters are the same as sample three in Table 2 because these already led to a consistent result. Each print consists of two samples (1 and 2 in Table 4) with a separation of 40 mm so the retraction is enabled when moving from one sample to another.

4.2.3.2 Results

It is noticeable in Table 4 that there is no consistency between the reprinted samples. One thing that can be remarked is that the second piece in the same print always has a higher resistivity than the first one. The overall resistance with a longer retraction distance leads to a higher resistance. It can be concluded that a higher retraction distance leads to a poor mixing ratio. The reason for this can be that the melted coating sticks to the guiding tubes when retracted, causing less conductive particles in the mixture that is extruded. The inconsistency of this result can be related to that of the previous section.

Retraction	Samples	A	B	C
2mm - 40mm/s	1	2,22 kΩ	2,08 kΩ	1,89 kΩ
	2	2,42 kΩ	2,51 kΩ	2,11 kΩ
20mm - 40mm/s	1	2,44 kΩ	2,02 kΩ	2,14 kΩ
	2	2,93 kΩ	2,11 kΩ	2,61 kΩ

Table 4: Results of different retraction distances

4.2.4 Extra investigation on printing temperature

The printing temperature (temperature of the nozzle) could have a huge impact on the mixing process of the material because it effects the viscosity of the material. For this reason, three sets of samples with respective 245, 250 and 265 degrees Celsius are printed in the next phase. The reason why the temperature lower than the standard 250 °C is only 5 degrees lower instead of 15 as the higher value of 265 °C, is because of the printability of the material. As mentioned in section 2.3, printing with a lower temperature led to printing errors and difficulties. The other fixed parameters are the same as sample three in Table 2 because these already led to a consistent result. Therefore, the results of sample three in Table 3 can be used for the samples printed with 250 °C. The same measurement methodology is used as in section 4.2.2.

4.2.4.1 Results

As shown in Table 5, it is evident that the printing temperature effects the resistivity of the material when extruded. The assumption made in 4.2.4 can be accepted: a higher printing temperature leads to a lower resistance, making the material more conductive. Consequently, a lower printing temperature leads to a higher resistance. It is a possibility that at higher temperatures, the material and coating mix better or structural changes within the material occur. It cannot be concluded that the material maintains a consistent conductivity across the same temperatures, the discrepancies among the samples are too significant.

Temperature	245 °C	250 °C	265 °C
A	3,23 kΩ	2,74 kΩ	1,63 kΩ
B	3,58 kΩ	2,62 kΩ	1,72 kΩ
C	3,07 kΩ	2,76 kΩ	1,35 kΩ

Table 5: Results of different printing temperatures

5 Design of Experiments

From the above studies, it can be concluded that the conductive FILAFLEX TPU has an irregular character. Due to the fact that this material is TPU, which is commonly known to be a material that is difficult to print with Bowden tubes (MakeShaper, 2016), this irregular character could be justified. To know the parameters that mainly influence the behavior of these types of conductive material, where the conductive particles are initially placed as an outer coating, it is interesting to perform a design of experiments (DoE).

A conductive PLA is selected for this purpose (Appendix 9). PLA is a material that is known to be easily printable (Liao et al., 2020). This filament has a diameter of 1.75 mm so the Ultimaker 3 Extended could not be used, this printer needs filament with a diameter of 2.85 mm. Therefore, the Creality cr-10 max printer is used (CR-10 Max | Creality Cloud, n.d.).

5.1 Testing parameters

Given the numerous factors influencing 3D print quality, the initial focus lies on examining different parameters. It would take too much time to examine all the parameters, so a selection of those to be examined is made based on previous studies. First, the study made in section 4 proves that the distance between the lines effects the conductivity whereas this forms the first parameter of the DoE. The different values of this parameter are as following: 0,8 mm (standard value with 0,8 mm nozzle), 0,7 mm and 0,6 mm. The decision is made to avoid selecting values higher than the standard, as doing so could lead to subpar connections between the various lines and consequently result in diminished quality.

Beniak et al. (2020) proves that the temperature of the nozzle has a considerable effect on the resistivity, which was also observed in section 4.2.4. It is noticed that with increasing print temperature, the measured conductivity is lower upon comparison of the measured values, a discrepancy of approximately 30% is observed. Thus, this constitutes the second variable. The different settings are as follows: 220°C, 235°C and 250°C.

Pejak Simunec & Sola (2022) demonstrates that conductivity, as measured by volume resistivity, exhibits strong anisotropy. This means that the conductivity varies significantly depending on whether the measurement is taken parallel or perpendicular to the layers. Specifically, when a printed cube was measured using probes placed perpendicular to the printed lines, it exhibited higher resistance compared to the same cube measured parallel to the printed lines. The difference in resistance was approximately 25%. Based on this information the final variable is accepted here, the layer print direction. A distinction is made between 0°, 45° and 90° relative to the print direction.

In order to reduce the number of experiments, a selection of infill pattern is made where an approximation of 100% density can be achieved. The walls (outer lines of the print) are eliminated, otherwise there would be a connection on the outside of the print while the conductivity through the different lines is needed to be investigated. Also, the other following parameters (Table 6) are considered as fixed:

Parameter	Value
Nozzle diameter	0,8 mm
Print speed	40 mm/s
Printbed temperature	60 °C
Material type	PLA (Appendix 9)
Infill type	Lines
Geometry	Figure 33

Table 6: Values of fixed parameter

As already mentioned, there are other some variables that need to be examined. The input variables of the design of experiments planned for this study are shown in Table 7. The amount and dispersion of the experiments are generated by “RStudio” software (Posit team, 2024) and are based on the input parameters consisting of three variables (line distance, printing temperature and layer direction) with each three values resulting in 27 samples. The code that is used to generate these experiments can be found in Appendix 10.

Nr	Line distance	Print temp	Layer direction	Nr	Line distance	Print temp	Layer direction
1	0.8 mm	220°C	0°	15	0.6 mm	235°C	45°
2	0.7 mm	220°C	0°	16	0.8 mm	235°C	90°
3	0.6 mm	220°C	0°	17	0.7 mm	235°C	90°
4	0.8 mm	220°C	45°	18	0.6 mm	235°C	90°
5	0.7 mm	220°C	45°	19	0.8 mm	250°C	0°
6	0.6 mm	220°C	45°	20	0.7 mm	250°C	0°
7	0.8 mm	220°C	90°	21	0.6 mm	250°C	0°
8	0.7 mm	220°C	90°	22	0.8 mm	250°C	45°
9	0.6 mm	220°C	90°	23	0.7 mm	250°C	45°
10	0.8 mm	235°C	0°	24	0.6 mm	250°C	45°
11	0.7 mm	235°C	0°	25	0.8 mm	250°C	90°
12	0.6 mm	235°C	0°	26	0.7 mm	250°C	90°
13	0.8 mm	235°C	45°	27	0.6 mm	250°C	90°
14	0.7 mm	235°C	45°				

Table 7: Amount and dispersion of experiments

5.2 Sample design

The design of the specimen (Figure 33) is a basic rectangular shape (easy to consistently modify the printing line direction) and a multiple of the preset layer height (0,2mm). Rounding of the corners (based on the nozzle diameter) are applied to improve the print speed and quality. One baseplate is designed for each set of specimens to print, with one fixed parameter whereas the other two variables can be changed for each individual specimen. This creates 3 base plates that will reduce printing time. This fixed parameter is the printing temperature whereas this parameter cannot be modified with the “per model setting” (explanation in section 3.2.3) for each individual specimen, shown in Figure 34. The measurement procedure is the same as in section 4.2.2.

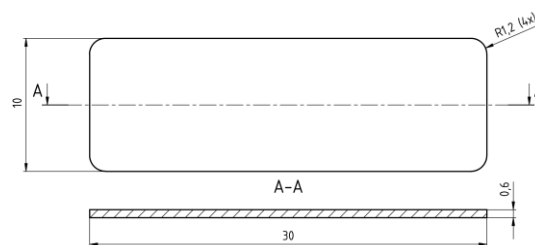


Figure 33: DoE sample design (dimensions in millimeters)

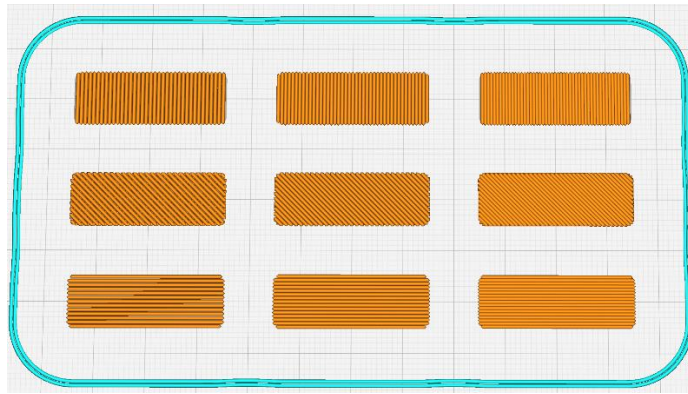


Figure 34: Visualization of "per model setting"

5.3 ANOVA study

ANOVA is a statistical method used to assess how a quantitative dependent variable varies based on the levels of one or more categorical independent variables. It evaluates whether there are differences in means among the groups at each level of the independent variable. Here, a three-way ANOVA test is used where the one dependent variable is the conductivity of the PLA. The effects of the parameters selected in 5.1 are determined using this test. These are the independent variables. The F-ratio assesses how effectively a set of independent variables explains the variability observed in the dependent variable. If that ratio is large enough, it can be concluded that not all means are equal. Only if the p-value is low enough (lower than 0.05), the variable is significant to be reported (Bevans, 2023).

5.3.1 Measurement

To obtain statistic correct results, every sample is printed and measured three times, and the average resistance is shown in Table 8.

Nr	Resistance (MΩ)	Nr	Resistance (MΩ)	Nr	Resistance (MΩ)
1	0.470	10	0.270	19	0.040
2	2.893	11	1.720	20	0.427
3	2.530	12	3.853	21	0.417
4	0.180	13	0.123	22	0.227
5	8.920	14	1.667	23	0.530
6	11.083	15	0.873	24	1.407
7	0.093	16	0.253	25	0.070
8	4.700	17	2.080	26	0.827
9	2.420	18	4.063	27	0.903

Table 8: Resistance of the samples

5.3.2 Statistic problems

The code to obtain the ANOVA study in the RStudio software can be found in Appendix 11. After running the code, the needed f-factor and p-value were not shown. This could be caused by three main reasons:

1. Missing Values: There might be missing values in the dataset, and the ANOVA function (aov) is unable to calculate the F and p-values for those cases.

2. Perfect Collinearity: The variables might be perfectly collinear, leading to numerical issues in the ANOVA computation.
3. Low Variability: There might be low variability in the data, leading to difficulties in estimating the parameters.

The collinearity test led to the conclusion that the variance inflation factors (VIFs) are all NaN (Not a Number), as shown in Figure 35, which indicates perfect collinearity between the variables. Perfect collinearity usually occurs when one variable can be accurately predicted using another variable or a combination of variables. If there is little variability within each combination, it can lead to perfect collinearity.

	GVIF	Df	GVIF ^{1/(2*Df)}
Temp	NaN	2	NaN
Direction	NaN	2	NaN
Distance	NaN	2	NaN
Temp:Direction	NaN	4	NaN
Temp:Distance	NaN	4	NaN
Direction:Distance	NaN	4	NaN
Temp:Direction:Distance	NaN	8	NaN

Figure 35: Result of collinearity test

It is noticeable in Table 8 that there is not always a lot of variability except for a few outliers. This could be explained by the printability of the Creality CR-10 max. This printer has a very big build plate (470 mm x 470 mm), resulting in an unstable surface for the material. A material has normally an ideal printing temperature, by manipulation this parameter, the print quality is affected. Therefore a three-way ANOVA analysis cannot be performed. Three independent one-way ANOVA tests will be conducted to examine the influence of the different variables.

5.3.3 Results

As already mentioned, the p-value of a variable needs to be lower than 0.5 for the variable to be significant. It is noticeable in Figure 36 that this value for the printing temperature and the line distance is lower. It can be assumed that these variables have a valuable impact on the conductivity of the samples based on these values.

	Df	Sum Sq	Mean Sq	F value	Pr(>F)		Df	Sum Sq	Mean Sq	F value	Pr(>F)
Temp	2	46.22	23.112	3.921	0.0336 *	Distance	2	43.22	21.61	3.589	0.0433 *
Residuals	24	141.47	5.895			Residuals	24	144.48	6.02		
Direction	2	9.39	4.694	0.632	0.54						
Residuals	24	178.31	7.429								

Figure 36: Results of one-way ANOVA studies

The visualization in Figure 37 shows the same result. When printing with a higher temperature, the resistivity of the material decreases, this was also found by Beniak et al. (2020). This phenomenon is explained in section 4.2.4.1.

The p-value of the direction is 0.54, which is higher than the accepted value resulting that the layer direction does not have a significant impact on the conductivity of this material. As shown in Figure 37, printing in a 0°- and 90°-angle results in a comparable value. Printing with a 45°-degree angle leads to a higher resistance. This could be explained by the connections between the printed lines. When the printer prints in horizontal or vertical lines only, only one stepper motor is activated to move the nozzle in one direction. When printing in a 45°-angle, the combination of two stepper motors is needed. This combination leads to an extra inaccuracy causing more printing difficulties. These line separations provide fewer contacts between printed lines, resulting in a higher resistance.

It is evident to see in Figure 37 that a smaller distance between the printed lines leads to a higher resistance. This is a remarkable singularity. It is expected that more material is mixed between two lines when the lines are printed closer to each other. Printing the lines closer to each other leads to more material in one single layer resulting in more material containing conductive particles. A characteristic of this material is that when more material is used in printing a sample, the quality declines. This reduced quality leads to increased resistance in the specimens.

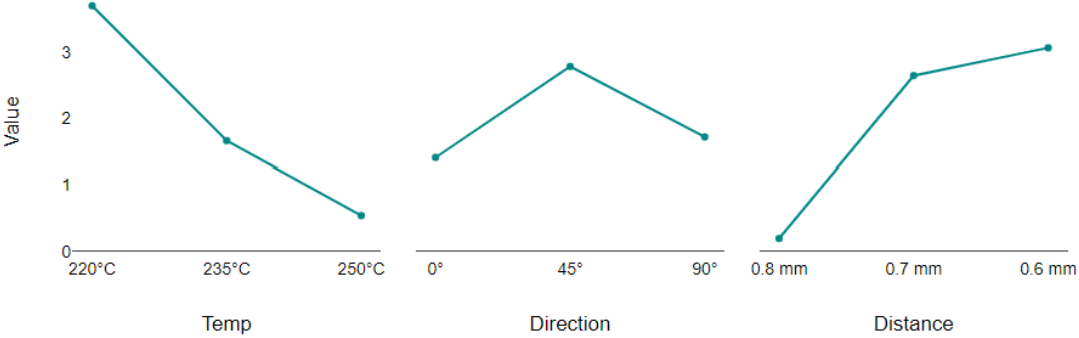


Figure 37: Visualization variables

6 Economic study and budget

In this section, a budget is made based on the costs associated with this project. The costs of materials, tests performed, licenses and workers' salaries will be analyzed.

6.1 Cost of used material

Table 9 shows the total cost of the material that is used to produce the samples for the applications, DoE, and carry on the tests. An estimate cost for the extra, small hardware components is also included in this table. Other hardware components as the Arduino Uno R3 or the MASTECH multimeter are not included in the calculation because these components were available from other projects.

Used material	Cost [€]
Recreus Conductive Filaflex	59,17
Recreus FilaFlex 82A original	26,67
PLA Conductive	19,61
Small hardware components (transistor, resistor, led...)	5
Total cost	110,45

Table 9: Cost of the used material

6.2 Cost of machines

6.2.1 Ultimaker 3 Extended

The new price of the Ultimaker 3 extended is € 3034,50. It is estimated that this machine will serve for five years while it will be used for of four months during this project. The calculation of what the machine costs for one hour is shown in equation (4).

$$A_m = \frac{E \cdot (1 + i)^a}{a \cdot H_a} \quad (4)$$

E = Ultimaker price (€3034,50)

i = annual bank interest rate (7% = 0,07)

a = number of years of printer life (5 years)

H_a = number of hours of printer use per year (200 hours)

This results in an hourly rate (A_m) of 4,26 €/h. During these four months, the printer printed in total for 35,53 hours resulting in a total of **€ 151,36**.

The Creality CR-10 Max is only used to print the samples for the design of experiments. This was only 2 hours of printing time so it can be included in the price of the Ultimaker.

6.2.2 Instron 5967

The Instron 5967 machine has an hourly rate of 30 €/h. This rate contains the tool setup, test preparation, cost of needed software, etc. This machine was used for two hours in total, resulting in a cost of **€ 60**.

6.2.3 NanoVNA h4

A Vector Network Analyzer was used to measure the return loss of the antenna. Therefore the NanoVNA h4 was purchased by the Mechanical and Materials department of the Universitat Politècnica de València. This machine has a new price of **€ 40,84**.

6.3 Cost of licenses

For the realization of this project, various licenses have been used: SolidWorks, MATLAB, Microsoft 365 (including Word, Excel and PowerPoint) and the Olympus microscope software. Licenses for SolidWorks, MATLAB and Microsoft 365 are provided by the Universitat Politècnica de València. They pay an amount each year for several licenses, making it difficult to determine a specific price for each license, which would be very low for one student. The Olympus microscope software is considered as amortized since it was acquired, together with the microscope, more than 10 years ago.

Other software as the Cura slicer and RStudio are free available applications without the need of a license.

6.4 Labor cost

The author of the work has been assigned the salary of a recently graduated engineer, corresponding with an hourly wage of € 25. This final degree project took around 280 hours of work for four months, resulting in a labor cost of **€ 7000**.

6.5 Total cost

Finally, the total cost for this project is calculated from the above costs and shown in Table 10. The total cost of this project is € 8908,81.

Type of cost	Cost [€]
Material	110,45
Machines	252,20
Licenses	-
Labor	7000
Contractual budget	7362,65
V.A.T. (21%)	1546,16
Total cost	8908,81

Table 10: Breakdown of project cost and total

Conclusion

In this final degree project, the applications of fused filament fabrication (FFF) with conductive materials were explored. By combining flexible conductive thermoplastic polyurethane (TPU) with traditional materials like PLA (Polylactic acid), the potential for low-cost prototyping in various domains were demonstrated. The experiments included creating strain gauges, antennas, and circuit boards using 3D printing technology. The outcomes of the applications became promising, and a suitable functionality was obtained after the iteration of parameters.

Based on this work, it can be concluded that conductive polymers exhibit highly unstable behavior, complicating the production of serial applications. Numerous factors influence the material's conductivity, including printing temperature, infill pattern, and material quantity. Furthermore, there are several other factors likely to have a significant impact that were not examined in this study and can be observed in further research.

The most notable issue that has been observed is the flexibility of the TPU. This is a material that is difficult to control, and this, combined with its conductive function, makes producing parts significantly more challenging. Obtaining a sufficient material flow in the print while ensuring good surface quality is challenging. This frequently led to retraction issues followed by obstructions in the extruder. Due to the lack of consistent reliability of the material, printing with conductive polymers is only recommended for applications where specific values do not need to be achieved or can be obtained through experimentation with trial and error. Despite challenges such as material behavior and operational problems, FFF remains a promising avenue for future research and practical applications in electronics and sensor technology.

Bibliography

- Abdulhussein, A. M., Khidhir, A. H., & Naser, A. A. (2021). 2.4 GHz Microstrip Patch Antenna for S-Band Wireless Communications. *Journal of Physics: Conference Series*, 2114(1), 012029. <https://doi.org/10.1088/1742-6596/2114/1/012029>
- Aloqalaa, Z. (2022). Electrically Conductive Fused Deposition Modeling Filaments: Current Status and Medical Applications. *Crystals*, 12(8), 1055. <https://doi.org/10.3390/cryst12081055>
- Beniak, J., Križan, P., & Matúš, M. (2015). A comparison of the tensile strength of plastic parts produced by a fused deposition modeling device. *Acta Polytechnica*, 55, 359–365. <https://doi.org/10.14311/AP.2015.55.0359>
- Beniak, J., Križan, P., & Matus, M. (2020). CONDUCTIVE MATERIAL PROPERTIES FOR FDM ADDITIVE MANUFACTURING. *MM Science Journal*, 2020(1), 3846–3851. https://doi.org/10.17973/MMSJ.2020_03_2019135
- Bevans, R. (2023, June 22). *ANOVA in R | A Complete Step-by-Step Guide with Examples*. Scribbr. <https://www.scribbr.com/statistics/anova-in-r/>
- Bilodeau, R. A., Miriyev, A., Lipson, H., & Kramer-Bottiglio, R. (2018). All-soft material system for strong soft actuators. *2018 IEEE International Conference on Soft Robotics (RoboSoft)*, 288–294. <https://doi.org/10.1109/ROBOSOFT.2018.8404934>
- Braza, J. (2020, May 18). How Voltage Dividers Work. *Circuit Basics*. <https://www.circuitbasics.com/what-is-a-voltage-divider/>
- Bureau, E. (2023, June 19). *Understanding Antenna Return Loss and VSWR with Formula*. <https://www.electronicsforu.com/technology-trends/antenna-return-loss-vswr>
- Castaneda, F. (2023, May 19). *Get started with Cura: Printing with two colors*. UltiMaker. <https://ultimaker.com/nl/learn/get-started-with-cura-printing-with-two-colors/>
- CR-10 Max | Creality Cloud. (n.d.). CR-10 Max | Creality Cloud. Retrieved May 15, 2024, from <https://www.crealitycloud.com>
- Cura: Ironing – Simply Explained*. (2024, March 17). All3DP. <https://all3dp.com/2/cura-ironing-3d-printing-ironing/>
- ER15—Heater error on PrintCore*. (2023, February 17). Ultimaker. <https://support.ultimaker.com/s/article/1667417565056>
- Fougeroux, T., Douyère, A., Murad, N. M., Sibille, J., Oree, S., & Dubard, J.-L. (2024). Performance enhancement of low-cost microstrip patch antennas through 3D-printed conductive geometric forms. *AEU - International Journal of Electronics and Communications*, 177, 155211. <https://doi.org/10.1016/j.aeue.2024.155211>
- Grellmann, H., Bruns, M., Lohse, F. M., Kruppke, I., Nocke, A., & Cherif, C. (2021). Development of an Elastic, Electrically Conductive Coating for TPU Filaments. *Materials*, 14(23), 7158. <https://doi.org/10.3390/ma14237158>
- Hullette, T. (2024, April 2). *Direct Drive vs Bowden Extruder: The Differences*. All3DP. <https://all3dp.com/2/direct-vs-bowden-extruder-technology-shootout/>
- Jaksic, N. I., & Desai, P. D. (2018). Characterization of resistors created by fused filament fabrication using electrically-conductive filament. *Procedia Manufacturing*, 17, 37–44. <https://doi.org/10.1016/j.promfg.2018.10.010>
- Liao, J., Brosse, N., Pizzi, A., Hoppe, S., Zhou, X., & Du, G. (2020). Characterization and 3D printability of poly (lactic acid)/acetylated tannin composites. *Industrial Crops and Products*, 149, 112320. <https://doi.org/10.1016/j.indcrop.2020.112320>
- Liu, H., Zhang, H., Han, W., Lin, H., Li, R., Zhu, J., & Huang, W. (2021). 3D Printed Flexible Strain Sensors: From Printing to Devices and Signals. *Advanced Materials*, 33(8), 2004782. <https://doi.org/10.1002/adma.202004782>
- MakeShaper. (2016, December 8). *Printing with Flexible 3D Filament*. Makeshaper. <https://www.makeshaper.com/post/printing-flexible-filament-things-to-consider>

- Maldonado, M. P., Pinto, G. M., Costa, L. C., & Fachine, G. J. M. (2022). Enhanced thermally conductive TPU/graphene filaments for 3D printing produced by melt compounding. *Journal of Applied Polymer Science*, 139(25), e52405. <https://doi.org/10.1002/app.52405>
- Maurizi, M., Slavič, J., Cianetti, F., Jerman, M., Valentinčič, J., Lebar, A., & Boltežar, M. (2019). Dynamic Measurements Using FDM 3D-Printed Embedded Strain Sensors. *Sensors*, 19(12), 2661. <https://doi.org/10.3390/s19122661>
- Misiak, M., Latko-Durałek, P., Baldy, E., Durałek, P., Górecka, Ż., Malmir, A., & Hatzikiriakos, S. G. (2024). Electrically conductive and flexible filaments of hot melt adhesive for the fused filament fabrication process. *Physics of Fluids*, 36(3), 037130. <https://doi.org/10.1063/5.0195103>
- Mitra, D., Roy, S., Striker, R., Burczek, E., Aqueeb, A., Wolf, H., Kabir, K. S., Ye, S., & Braaten, B. D. (2021). Conductive Electrified and Nonconductive NinjaFlex Filaments based Flexible Microstrip Antenna for Changing Conformal Surface Applications. *Electronics*, 10(7), 821. <https://doi.org/10.3390/electronics10070821>
- Out of Production 5900 Series Universal Testing Systems*. (n.d.). Retrieved May 3, 2024, from <https://www.instron.com/en/products/testing-systems/universal-testing-systems/low-force-universal-testing-systems/5900-series>
- Pejak Simunec, D., & Sola, A. (2022). Emerging Research in Conductive Materials for Fused Filament Fabrication: A Critical Review. *Advanced Engineering Materials*, 24(7), 2101476. <https://doi.org/10.1002/adem.202101476>
- Posit team. (2024). *RStudio: Integrated Development Environment for R* (2023.12.1.402) [Computer software]. Posit Software, PBC. <http://www.posit.co/>
- Ryan, K. R., Down, M. P., Hurst, N. J., Keefe, E. M., & Banks, C. E. (2022). Additive manufacturing (3D printing) of electrically conductive polymers and polymer nanocomposites and their applications. *eScience*, 2(4), 365–381. <https://doi.org/10.1016/j.esci.2022.07.003>
- S-Parameters for Antennas (S11, S12, ...)*. (n.d.). Retrieved April 30, 2024, from <https://www.antenna-theory.com/definitions/sparameters.php>
- Staff, E. (2020, June 5). *Why Strain Gauge Resistance Changes as it Stretches and Shrinks?* Inst Tools. <https://instrumentationtools.com/strain-gauge-resistance-changes/>
- Striker, R., Mitra, D., Braaten, B. D., Kabir, K. S., & Roy, S. (2020). On the Manufacturing Process of a Single-Step Fully 3D Printed Conformal Patch Antenna. *2020 IEEE International Conference on Electro Information Technology (EIT)*, 288–292. <https://doi.org/10.1109/EIT48999.2020.9208318>
- THE 17 GOALS | Sustainable Development*. (n.d.). Retrieved May 24, 2024, from <https://sdgs.un.org/goals>
- Ultimaker. (2021, January 7). *What is FFF 3D printing?* UltiMaker. <https://ultimaker.com/nl/learn/what-is-fff-3d-printing/>
- UltiMaker Cura*. (n.d.). UltiMaker. Retrieved April 9, 2024, from <https://ultimaker.com/software/ultimaker-cura/>
- UNO R3 | Arduino Documentation*. (n.d.). Retrieved April 11, 2024, from <https://docs.arduino.cc/hardware/uno-rev3/>
- Wang, C., Li, P., Xu, W., Song, L., & Huang, J. (2021). Tolerance analysis of 3D printed patch antennas based on interval arithmetic. *Microwave and Optical Technology Letters*, 63(2), 516–524. <https://doi.org/10.1002/mop.32605>
- What are antennas and how do they work? – TechTarget Definition*. (n.d.). Mobile Computing. Retrieved May 27, 2024, from <https://www.techtarget.com/searchmobilecomputing/definition/antenna>
- What are Load Cells and How Do They Work?* (n.d.). <https://www.omega.com/en-us/>. Retrieved March 4, 2024, from <https://www.omega.com/en-us/resources/load-cells>
- Wheatstone Bridge Circuit | Strain Gauge*. (n.d.). HBK World. Retrieved April 12, 2024, from <https://www.hbkworld.com/en/knowledge/resource-center/articles/strain-measurement-basics/strain-gauge-fundamentals/wheatstone-bridge-circuit>

List of appendices

Appendix 1: Datasheet Recreus conductive Filaflex.....	55
Appendix 2: Specifications Ultimaker 3 extended.....	56
Appendix 3: Datasheet MASTECH MS8221A.....	57
Appendix 4: Datasheet Recreus Filaflex 82A original.....	58
Appendix 5: Datasheet PA-1900/05 adapter.....	60
Appendix 6: Datasheet L7805C transistor.....	61
Appendix 7: Arduino code for voltage divider.....	62
Appendix 8: Matlab code for voltage divider.....	63
Appendix 9: Conductive PLA.....	65
Appendix 10: Code for dataset.....	66
Appendix 11: Code for ANOVA studies.....	67

Appendix 1: Datasheet Recreus conductive Filaflex



TECHNICAL DATA SHEET

CONDUCTIVE FILAFLEX

Description

CONDUCTIVE FILAFLEX is a Thermoplastic Polyurethane elastomer electrically conductive which makes it suitable for wearable devices and other flexible electronics applications. Thanks to its 92A shore hardness, it is compatible with 90% of the 3D printers on the market.

Physical Property	Value	Unit	Test method according to
Material density	1,330	g/cm ³	ISO 1183
	0,000	kg/m ³	ISO 1183
Melt flow rate (230°C/2.16kg)	12	g/10min	ISO 1133

Electrical Property	Value	Unit	Test method according to
Electrical resistivity surface	<6E1	ohm	ASTM D 257
Electrical resistivity	3,9 E3	ohm cm	

Thermal Property	Value	Unit	Test method according to
HDT (01,82MPa)	50	°C	ISO 75-2
VST Vicat Softening Temperature	50	°C	Vicat A Method: 10 Nw, 120°C/h

Conductive Property	Value	Unit	Test method according to
Dielectric factor 1MHz	6		IEC 62631-2-1
Dissipation factor, 100Hz	300	E-4	IEC 62631-2-1
Dissipation factor, 1MHz	950	E-4	IEC 62631-2-1
Volume resistivity	1E+10	Ohm*m	IEC 62631-3-1
Electric strength	35	kV/mm	IEC 60243-1
CTI Comparative tracking index	600		IEC 80112

Printing Properties	Recommended
Printing temperatures	245-250°C
Printing speed	20mm/s
Hot-bed temperature	50-60°C
Retractions	2-3mm/s to 40mm/s

Printing speed should be lower as recommended to get a perfect printing. After each change of material the extruder must be cleaned. To successfully use Conductive Filaflex filament in electronic applications, the electrical resistance of the circuit must be considered and it must take into account that this filament is designed for low current applications.

RECREUS INDUSTRIES S.L. VAT: ESB54876479
C/El Envelope, F13-F14, Pol. Ind. Finca Lacy
03600, Elda (Alicante) - SPAIN

(0034) 865 777 966
info@recreus.com
www.recreus.com

RECREUS INDUSTRIES S.L. Safety Data Sheet according to Regulation (EC) No.1907/2006 as amended from time to time.
Date / Revised: 24/10/2023 (REF 17042023)
Product: Conductive Filaflex

Appendix 2: Specifications Ultimaker 3 extended

Specifications

Printer and printing properties

Technology	Fused Deposition Modeling (FDM)
Print head	Dual extrusion print head with a unique auto-nozzle lifting system and swappable print cores
Build volume	Left nozzle: 215 x 215 x 300 mm Right nozzle: 215 x 215 x 300 mm Dual material: 197 x 215 x 300 mm
Filament diameter	2.85 mm
Layer resolution	0.4 mm nozzle: 20 - 200 micron
XYZ accuracy	12.5, 12.5, 2.5 micron
Print head travel speed	30 - 300 mm/s
Build speed	0.40 nozzle: up to 16 mm ³ /s
Build plate	Heated glass build plate
Build plate temperature	20 - 100 °C
Build plate leveling	Active leveling
Supported materials	Nylon, PLA, ABS, CPE, PVA
Nozzle diameter	0.4 mm
Nozzle temperature	180 - 280 °C
Nozzle heat up time	< 2 min
Build plate heat up time	< 4 min (20 - > 60 °C)
Operating sound	50 dBA
Material recognition	Material recognition with NFC scanner
Connectivity	Wi-Fi, LAN, USB port
Monitoring	Live camera

Physical dimensions

Dimensions	342 x 380 x 489 mm
Dimensions (with bowden tube and spool holder)	342 x 505 x 688 mm
Nett weight	11,3 kg
Shipping weight	16,8 kg
Shipping box dimensions	390 x 400 x 680 mm

Power requirements

Input	100 - 240V 4A, 50-60Hz 221 W max.
Output	24 V DC, 9.2 A

Ambient conditions

Operating ambient temperature	15 - 32 °C, 10 - 90% RH non condensing See material specifications for optimal conditions
Nonoperating temperature	0 - 32 °C

Software

Supplied software	Cura, our free print preparation software
Supported OS	macOS, Windows and Linux
File types	STL, OBJ and 3MF

Appendix 3: Datasheet MASTECH MS8221A

MASTECH®			MASTECH®																																				
3.2.1 DC Voltage <table border="1" style="width: 100%; border-collapse: collapse;"> <thead> <tr> <th>Range</th> <th>Resolution</th> <th>Accuracy</th> </tr> </thead> <tbody> <tr> <td>200mV</td> <td>0.1mV</td> <td rowspan="4" style="text-align: center;">±5.0% of rdg +1dgt</td> </tr> <tr> <td>2V</td> <td>1mV</td> </tr> <tr> <td>20V</td> <td>10mV</td> </tr> <tr> <td>200V</td> <td>100mV</td> </tr> <tr> <td>1000V</td> <td>1V</td> <td style="text-align: center;">±0.8% of rdg +2dgt</td> </tr> </tbody> </table> <p>Input impedance: 10MΩ Max. input voltage: 250Vdc or ac rms for 200mV range and 1000Vdc or peak ac for other ranges.</p>			Range	Resolution	Accuracy	200mV	0.1mV	±5.0% of rdg +1dgt	2V	1mV	20V	10mV	200V	100mV	1000V	1V	±0.8% of rdg +2dgt	Overload protection:F200mA/250V fuse (10A range unfused). Max. input current: mA: 200mA dc or 200mA ac rms 10A: 10A continuous, 20A 15 sec. MAX.																					
Range	Resolution	Accuracy																																					
200mV	0.1mV	±5.0% of rdg +1dgt																																					
2V	1mV																																						
20V	10mV																																						
200V	100mV																																						
1000V	1V	±0.8% of rdg +2dgt																																					
3.2.2 AC Voltage <table border="1" style="width: 100%; border-collapse: collapse;"> <thead> <tr> <th>Range</th> <th>Resolution</th> <th>Accuracy</th> </tr> </thead> <tbody> <tr> <td>2V</td> <td>1mV</td> <td rowspan="3" style="text-align: center;">±0.8% of rdg +3dgt</td> </tr> <tr> <td>20V</td> <td>10mV</td> </tr> <tr> <td>200V</td> <td>100mV</td> </tr> <tr> <td>750V</td> <td>1V</td> <td style="text-align: center;">±1.2% of rdg +3dgt</td> </tr> </tbody> </table> <p>Input impedance: 10MΩ Max. input voltage: 250Vdc or ac rms for 200mV range and 1000Vdc or 750V ac rms for other ranges, Frequency Range: 4 0Hz-1kHz; Indication: Average (rms of sine wave)</p>			Range	Resolution	Accuracy	2V	1mV	±0.8% of rdg +3dgt	20V	10mV	200V	100mV	750V	1V	±1.2% of rdg +3dgt	3.2.4 AC Current <table border="1" style="width: 100%; border-collapse: collapse;"> <thead> <tr> <th>Range</th> <th>Resolution</th> <th>Accuracy</th> </tr> </thead> <tbody> <tr> <td>2mA</td> <td>1μA</td> <td style="text-align: center;">±1.2% of rdg +3dgt</td> </tr> <tr> <td>20mA</td> <td>10μA</td> <td rowspan="2" style="text-align: center;">±2.0% of rdg +3dgt</td> </tr> <tr> <td>200mA</td> <td>0.1mA</td> </tr> <tr> <td>10A</td> <td>10mA</td> <td style="text-align: center;">±3.0% of rdg +7dgt</td> </tr> </tbody> </table> <p>Overload protection:F200mA/250V fuse (10A range unfused). Max. input current: mA: 200mA dc or 200mA ac rms 10A: 10A continuous, 20A 15 sec. MAX Frequency Range: 40Hz-1kHz; Indication: Average (rms of sine wave)</p>			Range	Resolution	Accuracy	2mA	1μA	±1.2% of rdg +3dgt	20mA	10μA	±2.0% of rdg +3dgt	200mA	0.1mA	10A	10mA	±3.0% of rdg +7dgt							
Range	Resolution	Accuracy																																					
2V	1mV	±0.8% of rdg +3dgt																																					
20V	10mV																																						
200V	100mV																																						
750V	1V	±1.2% of rdg +3dgt																																					
Range	Resolution	Accuracy																																					
2mA	1μA	±1.2% of rdg +3dgt																																					
20mA	10μA	±2.0% of rdg +3dgt																																					
200mA	0.1mA																																						
10A	10mA	±3.0% of rdg +7dgt																																					
3.2.3 DC Current <table border="1" style="width: 100%; border-collapse: collapse;"> <thead> <tr> <th>Range</th> <th>Resolution</th> <th>Accuracy</th> </tr> </thead> <tbody> <tr> <td>200μA</td> <td>0.1μA</td> <td rowspan="3" style="text-align: center;">±0.8% of rdg +1dgt</td> </tr> <tr> <td>2mA</td> <td>1μA</td> </tr> <tr> <td>20mA</td> <td>10μA</td> </tr> <tr> <td>200mA</td> <td>0.1mA</td> <td style="text-align: center;">±1.2% of rdg +1dgt</td> </tr> <tr> <td>10A</td> <td>10mA</td> <td style="text-align: center;">±2.0% of rdg +5dgt</td> </tr> </tbody> </table>			Range	Resolution	Accuracy	200μA	0.1μA	±0.8% of rdg +1dgt	2mA	1μA	20mA	10μA	200mA	0.1mA	±1.2% of rdg +1dgt	10A	10mA	±2.0% of rdg +5dgt	3.2.5 Resistance <table border="1" style="width: 100%; border-collapse: collapse;"> <thead> <tr> <th>Range</th> <th>Resolution</th> <th>Accuracy</th> </tr> </thead> <tbody> <tr> <td>200Ω</td> <td>0.1Ω</td> <td style="text-align: center;">±0.8% of rdg +3dgt</td> </tr> <tr> <td>2kΩ</td> <td>1Ω</td> <td rowspan="4" style="text-align: center;">±0.8% of rdg +1dgt</td> </tr> <tr> <td>20kΩ</td> <td>10Ω</td> </tr> <tr> <td>200kΩ</td> <td>100Ω</td> </tr> <tr> <td>2MΩ</td> <td>1kΩ</td> </tr> <tr> <td>20MΩ</td> <td>10kΩ</td> <td style="text-align: center;">±1.0% of rdg +2dgt</td> </tr> </tbody> </table> <p>Overload protection: 250V dc or 250Vac rms.</p>			Range	Resolution	Accuracy	200Ω	0.1Ω	±0.8% of rdg +3dgt	2kΩ	1Ω	±0.8% of rdg +1dgt	20kΩ	10Ω	200kΩ	100Ω	2MΩ	1kΩ	20MΩ	10kΩ	±1.0% of rdg +2dgt
Range	Resolution	Accuracy																																					
200μA	0.1μA	±0.8% of rdg +1dgt																																					
2mA	1μA																																						
20mA	10μA																																						
200mA	0.1mA	±1.2% of rdg +1dgt																																					
10A	10mA	±2.0% of rdg +5dgt																																					
Range	Resolution	Accuracy																																					
200Ω	0.1Ω	±0.8% of rdg +3dgt																																					
2kΩ	1Ω	±0.8% of rdg +1dgt																																					
20kΩ	10Ω																																						
200kΩ	100Ω																																						
2MΩ	1kΩ																																						
20MΩ	10kΩ	±1.0% of rdg +2dgt																																					
07			08																																				

Appendix 4: Datasheet Recreus Filaflex 82A original



TECHNICAL DATA SHEET

FILAFLEX 82A ORIGINAL

Description

Filaflex is a Thermoplastic Polyether-Polyurethane elastomer with additives that allow high printability in FDM printers. Filaflex® has a remarkable hydrolysis resistance, high resistance to bacteria and low temperature flexibility properties in printed parts.

Physical Property	Value	Unit	Test method according to
Material density	1,120	g/cm ³	ISO 1183
	1120,000	kg/m ³	ISO 1183
Melt flow rate (230°C/2,16kg)	0,000	g/10min	ISO 1133

Mechanical Property	Value	Unit	Test method according to
Tensile modulus (Young)	22,00	MPa	ISO 527
Tensile strength	45	MPa	DIN 53504-S2
Elongation at break	650,00	%	DIN 53504-S2
Stress at 20% elongation	2,50	MPa	DIN 53504-S2
Stress at 100% elongation	6,00	MPa	DIN 53504-S2
Stress at 300% elongation	10,00	MPa	DIN 53504-S2
Tear strength	70,00	N/mm	ISO 34-1
Abrasion resistant	25,00	mm ³	ISO 4649
Compression set 23°C/72 hours	25,00	%	ISO 815
Compression set 70°C/24 hours	45,00	%	ISO 815
Tensile strength after storage in water at 80°C for 42	32,00	Mpa	DIN 53504-S2
Elongation at break after storage in water at 80°C for	600,00	%	DIN 53504-S2
Notched impact strength (Charpy)n at +23°C	nb	kJ/m ²	ISO 179
Notched impact strength (Charpy)n at -30°C	nb	kJ/m ²	ISO 179
Tensile notched impact strength, +23°C	580,00	kJ/m ²	ISO 8256/1

Thermal Property	Value	Unit	Test method according to
Combustibility O2 index	23,0	%	ISO 4589-1/-2
Burning behaviour	HB	CLASS	UL 94
Yellow Card Available	yes		
Glass Transition Temperature 10°C/min	-42,0	°C	ISO 11357-1/-2
VST Vicat Softening Temperature	113,0	°C	Vicat A Method: 10 Nw, 120°C/h
Thermal Conductivity	0,3	W/(mK)	DIN 52612-1
Coefficient Thermal Expansion at 23°C	210,0	1/K	ISO 11359-2

Conductive Property	Value	Unit	Test method according to
WDD Water Vapor Permiability	17,00	g/m2d	ISO 15106-2
Electrical resistivity surface	0	ohm	ASTM D 257
Electrical resistivity	1E+10	ohm cm	
Electrical conductivity	0	ohm-1 cm-1	
Dielectric factor 100Hz	0		IEC 62631-2-1
Dielectric factor 1MHz	6		IEC 62631-2-1
Dissipation factor, 100Hz	300	E-4	IEC 62631-2-1
Dissipation factor, 1MHz	950	E-4	IEC 62631-2-1
Volume resistivity	1E+10	Ohm*m	IEC 62631-3-1
Electric strength	35	kV/mm	IEC 60243-1
CTI Comparative tracking index	600		IEC 60112

Printing properties	Recommended
Printing temperatures	215 - 250°C
Printing speed	20 - 60 mm/s
Hot-bed temperature	0°C
Optimal layer height	0.2 mm
Minimal nozzle diameter	0.4 mm or higher
Retraction parameters	3.5 - 6.5 mm (speed 20 - 160 mm/s)

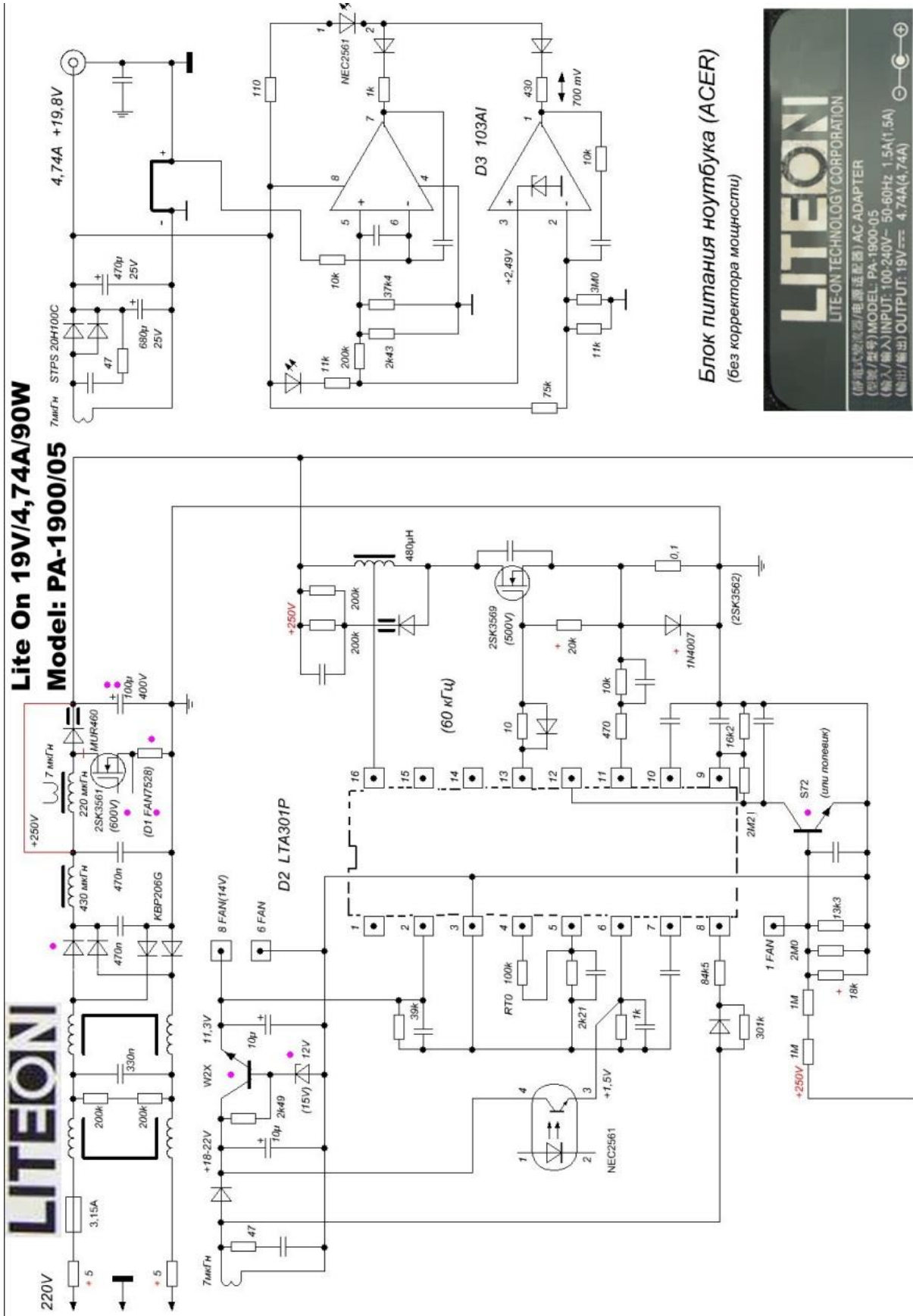
RECREUS INDUSTRIES S.L. VAT: ESB54876479
 C/EI Envelope, F13-F14, Pol. Ind. Finca Lacy
 03600, Elda (Alicante) - SPAIN

(0034) 865 777 966
 info@recreus.com
 www.recreus.com

RECREUS INDUSTRIES S.L. Safety Data Sheet according to Regulation (EC) No. 1907/2006 as amended from time to time.

Date / Revised: 20.10.2021
 Product: Filaflex 82A Original

Appendix 5: Datasheet PA-1900/05 adapter



Appendix 6: Datasheet L7805C transistor

Table 10. Electrical characteristics of L7805C

Symbol	Parameter	Test conditions	Min.	Typ.	Max.	Unit
V_O	Output voltage	$T_J = 25\text{ }^\circ\text{C}$	4.8	5	5.2	V
V_O	Output voltage	$I_O = 5\text{ mA to }1\text{ A}, V_I = 7\text{ to }18\text{ V}$	4.75	5	5.25	V
V_O	Output voltage	$I_O = 1\text{ A}, V_I = 18\text{ to }20\text{ V}, T_J = 25\text{ }^\circ\text{C}$	4.75	5	5.25	V
ΔV_O ⁽¹⁾	Line regulation	$V_I = 7\text{ to }25\text{ V}, T_J = 25\text{ }^\circ\text{C}$		3	100	mV
		$V_I = 8\text{ to }12\text{ V}, T_J = 25\text{ }^\circ\text{C}$		1	50	
ΔV_O ⁽¹⁾	Load regulation	$I_O = 5\text{ mA to }1.5\text{ A}, T_J = 25\text{ }^\circ\text{C}$			100	mV
		$I_O = 250\text{ to }750\text{ mA}, T_J = 25\text{ }^\circ\text{C}$			50	
I_d	Quiescent current	$T_J = 25\text{ }^\circ\text{C}$			8	mA
ΔI_d	Quiescent current change	$I_O = 5\text{ mA to }1\text{ A}$			0.5	mA
		$V_I = 7\text{ to }23\text{ V}$			0.8	
$\Delta V_O/\Delta T$	Output voltage drift	$I_O = 5\text{ mA}$		-1.1		mV/°C
eN	Output noise voltage	$B = 10\text{ Hz to }100\text{ kHz}, T_J = 25\text{ }^\circ\text{C}$		40		$\mu\text{V}/V_O$
SVR	Supply voltage rejection	$V_I = 8\text{ to }18\text{ V}, f = 120\text{ Hz}$	62			dB
V_d	Dropout voltage	$I_O = 1\text{ A}, T_J = 25\text{ }^\circ\text{C}$		2		V
R_O	Output resistance	$f = 1\text{ kHz}$		17		m Ω
I_{sc}	Short circuit current	$V_I = 35\text{ V}, T_J = 25\text{ }^\circ\text{C}$		0.75		A
I_{scp}	Short circuit peak current	$T_J = 25\text{ }^\circ\text{C}$		2.2		A

1. Load and line regulation are specified at constant junction temperature. Changes in V_O due to heating effects must be taken into account separately. Pulse testing with low duty cycle is used.

Appendix 7: Arduino code for voltage divider

```
void setup() {  
  Serial.begin(9600);  
}  
  
void loop() {  
  int sensorValue = analogRead(A0);  
  Serial.println(sensorValue);  
  delay(1000); // Delay to not overload the CPU  
}
```

Appendix 8: Matlab code for voltage divider

```
% Delete existing serial connections on COM3
delete(instrfind({'Port'},{'COM3'}));

% Open a serial connection to the Arduino
serialPort = 'COM3'; %Matches Arduino's COM port
baudRate = 9600;
arduino = serial(serialPort, 'BaudRate', baudRate);
fopen(arduino);
X_Value = [];
Y_Value = [];
i = 1;

% Initialize keyboard interrupt
desktop = com.mathworks.mde.desk.MLDesktop.getInstance;
cw = desktop.getClient('Command Window');
xCmdWndView = cw.getComponent(0).getViewport.getComponent(0);
h_cw = handle(xCmdWndView, 'CallbackProperties');
set(h_cw, 'KeyPressedCallback', @CmdWinKeyCallback);
CmdWinKeyCallback('reset');

try
    tic; % Start the timer
    while true
        % Read analog input from Arduino
        fprintf(arduino, 'R');
        data = fscanf(arduino, '%d');
        voltage = data*(5/1023); %Factor to transfer analog input to digital
        R2 = 214; %Known resistor
        Resistance = R2*((5-voltage)/voltage); %Voltage divider formula to calculate
resistance

        % Calculate elapsed time in seconds
        time_seconds = toc;
        time_seconds = round(time_seconds,1);
        % Display the current resistor value and timestamp for monitoring
        disp(['Time (s): ', num2str(time_seconds), ', Resistor Value: ',
num2str(Resistance)]);

        % Write X_Value and Y_Value to the text file with comma decimal separator
        X_Value(i) = time_seconds;
        Y_Value(i) = Resistance;

        % Check for keyboard interrupt
        if CmdWinKeyCallback()
            disp('Esc key pressed. Stopping...');
            break
        end

        i = i + 1;
        % Pause here to control the loop speed (accuracy of the plot)
        pause(1);
    end
catch
    fclose(arduino); % Close the serial connection when done or in case of an error
end

% Save data to an Excel file
data_matrix = [X_Value', Y_Value']; % Concatenate X_Value and Y_Value as columns
xlswrite('resistor_values.xlsx', data_matrix);

% Plot the graph
plot(X_Value, Y_Value);
hold on;
```



```

xlabel('Time (s)');
ylabel('Resistance (\Omega)');
title('Resistance in function of Time');
grid on;

% Keyboard interrupt function
function Value = CmdWinKeyCallback(~, eventdata)
    persistent KeyPressed
    switch nargin
        case 0
            Value = ~isempty(KeyPressed);
        case 1
            KeyPressed = [];
        case 2
            if eventdata.getKeyCode() == 27 % 27 = 'Esc'
                KeyPressed = true;
            else
                KeyPressed = [];
            end
        otherwise
            error('Programming error');
    end
end
end

```

Appendix 9: Conductive PLA

Conductive PLA Filament Replacement 3D Printer Accessory 1.75mm Printing Consumable 20 50mm/s

Characteristic:

1. CONDUCTIVE MATERIAL: This conductive filament becomes a conductive material by combining PLA with conductive materials such as carbon or graphene.
2. GOOD DURABILITY: This conductive PLA filament has better durability and wear resistance than other materials, it can withstand multiple tests and uses.
3. RESISTIVITY OF 1.42 Ω cm: The resistivity of this conductive PLA filament is 1.42 Ω cm, suitable for use as an electrical track for LED joystick and other small devices.
4. PRINTING PARAMETERS: The printing speed of 1.75mm PLA filament is 20 50mm/s, and the printing temperature is 220-250°C, which is safe and practical.
5. WIDE APPLICATION: The conductive 3D printer consumable can be used for keychains, LED gloves and even automatic bed leveling projects.

Specification:

Item Type: 1.75mm Filament

Material: PLA

Printing Temperature: 220-250°C

Printing Speed: 20-50mm/s

Appendix 10: Code for dataset

```
# Install and load the skpr package
install.packages("skpr")
library(skpr)
# Make the dataset
FirstSample_set = expand.grid(LineDistance = c("0.8 mm", "1 mm", "1.2 mm"), PrintTemp = c("220°C", "235°C", "250°C"),
LayerDirection = c("0°", "45°", "90°"))
# Load the dplyr package
library(dplyr)
# Sort the sample set by PrintTemp
FirstSample_set_sorted <- arrange(FirstSample_set, PrintTemp)
# Install and load the xlsx package
install.packages("openxlsx")
library(openxlsx)
# Sort the sample set by PrintTemp
FirstSample_set_sorted <- arrange(FirstSample_set, PrintTemp)
# Define the file path and name for the Excel file
file_path<-"C:/Users/rondo/OneDrive/ODISEE/Documenten/Odisee/UPV/Statistics/sorted_sample_set.xlsx"
# Write the sorted sample set to an Excel file using openxlsx
write.xlsx(FirstSample_set_sorted, file_path)
# Confirmation message
cat("Sorted sample set has been saved as 'sorted_sample_set.xlsx'")
```

Appendix 11: Code for ANOVA studies

a) Three-way ANOVA with collinearity and variability tests

```
# Load necessary libraries
library(tidyverse)
library(car)

# Load the dataset
Data<-read.csv("C:/Users/rondo/OneDriveODISEE/Documenten/Odisee/UPV/Statistics/DATASETANOVA.CSV")
data$Temp <- as.factor(data$Temp)
data$Direction <- as.factor(data$Direction)
data$Distance <- as.factor(data$Distance)

# Check for missing values
summary(data)

# Check for collinearity
collinearity <- vif(lm(Value ~ Temp * Direction * Distance, data = data))
print(collinearity)

# Check for variability
boxplot(Value ~ Temp * Direction * Distance, data = data)

# Perform three-way ANOVA
anova_result <- aov(Value ~ Temp * Direction * Distance, data = data)

# Display ANOVA results
summary_table <- summary(anova_result)
print(summary_table)
```

b) One-way ANOVA tests

```
# Load necessary libraries
library(tidyverse)
library(car)

# Load the dataset
data<-
read.csv("C:/Users/rondo/OneDriveODISEE/Documenten/Odisee/UPV/Statistics/DATASETANOVAONLYTEMP.CSV")
data$Temp <- as.factor(data$Temp)
str(data)
summary(data)

# Perform three-way ANOVA
anova_result <- aov(Value ~ Temp , data = data)
print(summary(anova_result))
```

The same for ONLYDISTANCE.CSV and ONLYDIRECTION.CSV, with the with the necessary replacements of "Temp".